Emerging roles of deoxynucleotide metabolism in genotoxic stress tolerance

In the foreword, I wish to say that we have carried out all the planned experiments with publication quality results as an outcome. Along the way we met several difficulties that had to be overcome in order to stick to the project aims. Due to these difficulties, we lag behind our original publication schedule. We are now in the process of preparing several manuscripts in parallel from data acquired during the project period (OTKA rules allow the joining of prospective publications the final report of the grant later on). Therefore, this report is a relatively long one aiming at presenting the data in a publication-like manner. On the other hand, thanks to the same difficulties we encountered, we published valuable papers driven by the need for methodological development [1–3] and are in the process of publishing more in this matter.

Before we started the project, it had long been evident that a fine-tuned and well conserved concentration balance in the pool of deoxyribonucleoside 5'-triphosphates (deoxynucleotides or dNTPs) was necessary to maintain the normal cell cycle and the integrity of the genome. Based on our previous results, we became interested in the relation of dNTP pool homeostasis to the emergence of drug resistance in *Mycobacteria*, including *Mycobacterium tuberculosis* (*Mtb*), the causative agent of tuberculosis. *Mtb* develops drug resistance exclusively by single-nucleotide mutations [4]. Interestingly, the basal mutation rate in mycobacteria is very low *in vitro*, it is estimated that the organism makes a mutational error at two bases in every 10 000 genomes copied [5]. However, isolates from patients display a remarkable genomic diversity including several different drug resistant strains even in the same isolate [6]. The discrepancy between the *in vitro* and *in vivo* observations suggested us that genotoxic stress factors within the host may elicit increased mutation rates by unknown mechanisms. Systematic studies on dNTP pool regulation linking endogenous and environmental stresses to dNTP pool changes and in turn to DNA repair were missing. Therefore, we **created the hypothesis that environmental stress factors alter the dNTP pool in mycobacteria and promote erroneous DNA repair and mutagenesis that results in stress tolerance. If the environmental stress factors are tuberculosis drugs, adaptation to stress is drug resistance. We thought that the understanding of the interrelations of these processes would help understanding the mechanism of drug resistance and would allow better management of current therapeutics.**

We chose *Mycobacterium* as a model system for several reasons. First, intracellular mycobacterial pathogens are exposed to harsh genotoxic conditions as part of the immune response. It is therefore of major importance for these bacteria to develop strategies for the adaptation to genotoxic environmental conditions. Secondly, the metabolic pathways leading to dNTP production are well separated from other metabolic routes, e.g. dTTP synthesis occurs exclusively through dUTP breakdown and are conserved within the *Mycobacterium* genus. Salvage pathways for thymine or thymidine are not present. Thirdly, mycobacteria lack genes encoding for mismatch repair (MMR) [7]. An operating MMR would hinder the analysis of the mutational spectrum arising from dNTP pool changes [8]. And last but not least, the biomedical relevance of this model system lies in that tuberculosis represents one of the largest medical challenges worldwide due to the emergence of extremely (XDR-TB) and totally (TDR-TB) drug-resistant strains [9].

Aim 1 Establish the relationship between the exposure to environmental stress and the changes in size and balance of the cellular dNTP pool in *Msm*

To achieve this goal, we needed to precisely measure dNTP concentrations in a large number of biological samples. As several methods were available to quantify dNTPs, we did not expect running into a major problem right at the start line. Especially because the measurement of cellular dNTP pools is gaining increasing significance nowadays due to its involvement in tumorigenesis, aging, cell cycle control and antiviral defense. The two main techniques available were i) high performance liquid chromatography (HPLC) methods or ii) DNA polymerization based enzymatic assays. The HPLC based techniques can be coupled with either UV or mass spectrometry (MS) detection. But both methods require well equipped, specialized laboratories and high level of analytical expertise due to the difficulties of separating dNTPs from chemically hardly distinguishable NTPs present in 100-1000X amounts in the cells. We set up a collaboration with an expert in analytics and tried to apply the HPLC-MS method. We stopped the trials after 2 years full of difficulties with the instruments. In parallel with the HPLC-MS measurements, we started to apply the most promising DNA polymerization-based method available at that time. It had the advantage of high specificity and high sensitivity, as well as the possibility to make it streamlined. This fluorescence-based assay utilizes the 5'-3' exonuclease activity of Taq polymerase so that when polymerization reaches the fluorescently-labeled probe, after the incorporation of certain number of dNTP analyte, Taq polymerase hydrolyzes it, and the fluorescence signal is released from the quenching [1]. Unfortunately, the assay did not work as published and we found ourselves unable to measure dNTP levels.

We realized that any easily accessible method existed to measure dNTPs in a standard molecular biology laboratory. We therefore set out to resolve the difficulties with the fluorescence-based dNTP assay for ourselves and for the scientific community. We identified the sources of the background signals that made the evaluation of the dNTP incorporation time courses impossible and applied a kinetic treatment to decouple the disturbing background from the signal proportionate to the analyte dNTP incorporation. We wished to offer a user-friendly method for an average user, and thus, we implemented our evaluation algorithm into the software "nucleoTIDY". nucleoTIDY can complete the full kinetic evaluation process generating the final dNTP amounts from raw fluorescence curves recorded by the qPCR instrument in 96-well-plates. Several checkpoints were built into the software, so even unexperienced users can rely on the results. nucleoTIDY saves significant time and effort for the users and is freely available at http://nucleotidy.enzim.ttk.mta.hu/. All in all, the development of this dNTP quantification assay became one of the achievements of this project which we published in Nucleic Acids Research[1].

While struggling with dNTP measurements, we were implementing the planned stress treatments on *Msm*. What treatments and why these did we choose? We attempted to model stresses that this pathogen encounters during its life cycle. Tuberculosis spreads in the air with droplets where it is exposed to UV light. When the pathogen enters the body, it encounters the immune system. Endocytically competent alveolar macrophages take up the pathogen. The trick of *Mtb* is that it prevents the fusion of its residence endosome with lysosomes and therefore, it is able to stay in nonacidified vacuoles. Nevertheless, the immune cells attack the unwanted intruder by reactive oxygen and nitrogen compounds and by a shortage of nutrients. Antituberculotics represent a longstanding stress factor as well. The standard treatment of tuberculosis is a 6-months long therapy

with four of the first-line drugs (rifampicin, isoniazid, ethambutol and pyrazinamide) used in combination. Although the curation is successful in 85% of the cases, the improper use of antibiotics often results in antibiotic resistance development. The MDR-TB strains are resistant at least to the two most effective tuberculosis drugs, to rifampicin and isoniazid. The therapy of patients with MDR-TB can be achieved by second-line antibiotics (e.g. fluoroquinolones, amikacin). However, these drugs are often more toxic and expensive and the treatments with them needs even more time (2 years) with a lower success rate (56%)[9]. Extensively or totally drug-resistant tuberculosis (XDR-TB) cases are resistant to any fluoroquinolones and another second-line antibiotics besides being resistant to rifampicin and isoniazid[10,11].

Thus, we identified UV radiation and nutrient starvation as environmental stress factors and the following stress factors that affect the bacteria in a host: nutrient starvation, hypoxia, alkylation, reactive oxygen species (ROS), reactive nitrogen intermediates (RNI), first-line and second-line antibiotics. We wished to study these effects systematically. For that reason, we generated these stress conditions separately to decipher to which extent these contribute to dNTP pool changes and an increased mutagenesis rate. To establish the stress conditions, we designed the experiment parameters: time and concentration. Determining the duration of the treatments was based on the growth curve of *Msm* cells (**Figure 1A**). It is visible, that the exponential phase of the growth curve occurs from OD_{600} of 0.1 to 0.8. This growth phase takes 18 hours. Interestingly, in our pilot experiments, we observed differences in the level of dNTPs when cultures with different OD_{600} values were measured. To establish a reproducible range of growth for the overall experimentation, we measured dNTP levels of the differential stages of the growth curve of non-treated bacteria (**Figure 1B**).

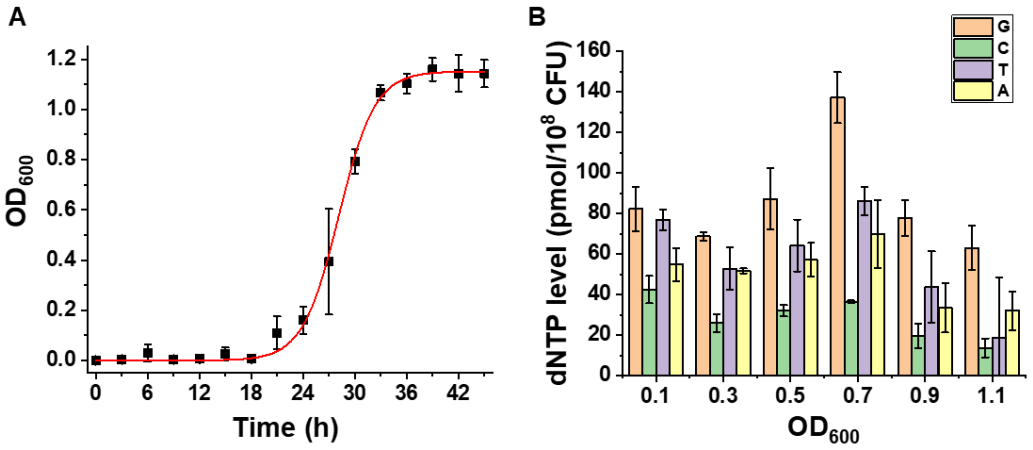

Figure 1: dNTP pool changes in function of the growth states in *Msm*. A) The growth curve of *M. smegmatis* measured by OD_{600}. Scatter plots represent the average of 3 different *Msm* cultures, error bars are standard deviations. The red line represents fitting of the data with $y = \frac{a}{1+e^{-k(x-x_c)}}$ equation; the following parameters were yielded: a = 1.15 ± 0.02, k = 0.48 ± 0.03, x_c = 28.13 ± 0.25. **B) dNTP levels of *Msm* in function of the optical density of the cell culture**

The highest level of the dNTPs was measured at OD_{600} 0.7, in the middle of the exponential growth phase, while the lowest level was measured at OD_{600} 1.1, when the culture reaches saturation. At the beginning of exponential growth, we measured dNTP levels between 25-90 pmol/10^8 CFU and is somewhat fluctuating. It is important to note, that the pattern of the four dNTPs are the same in all measured cases, with dGTP concentration being the highest and dCTP concentration being the lowest of the four (dGTP>dTTP>dATP>dCTP). This observation suggests that this precise ratio of the four dNTPs is needed for proper DNA replication. To standardize our stress treatments, we decided to begin the treatments with growing cultures at OD_{600} 0.1. Our aim was to treat as much generation as possible, but we aimed to avoid reaching the saturation of growth. For that reason, we defined the duration of every treatment to be 8 hours (with a few exceptions). In this case, non-treated ('control') cultures will reach the maximum level of dNTP at the end of the experiments.

To determine the concentration of the substances to be used for the treatments, we applied a wide range of concentrations of every substance based on literature data. We searched for the concentration that enabled some growth of the *Msm* cells, i.e. is not completely lethal for the culture. This was important in order to isolate dNTPs after the treatment. The experimentally chosen final conditions for the applied stress treatments are summarized in **Table 1**.

Stress treatment	**Applied condition (8h treatment if not otherwise specified)**
UV irradiation	65 J, instantaneous
Dormancy	0.4% glucose
Mitomycin-C	0.01 µg/ml
$NaNO_2$	5 mM
Hypoxia	Microaerofil bags for plates or cutting oxygen supply in shaker cultures for 16 hours
Rifampicin	3 µg/ml
Isoniazid	150 µg/ml
Ethambutol	100 µg/ml
Ciprofloxacin	0.3 µg/ml
Clofazimine	5 µg/ml

Table 1: Stress conditions used to treat *M. smegmatis* cells

The effect of each treatment on *Msm* cultures is shown in **Figures 2** and **3**.

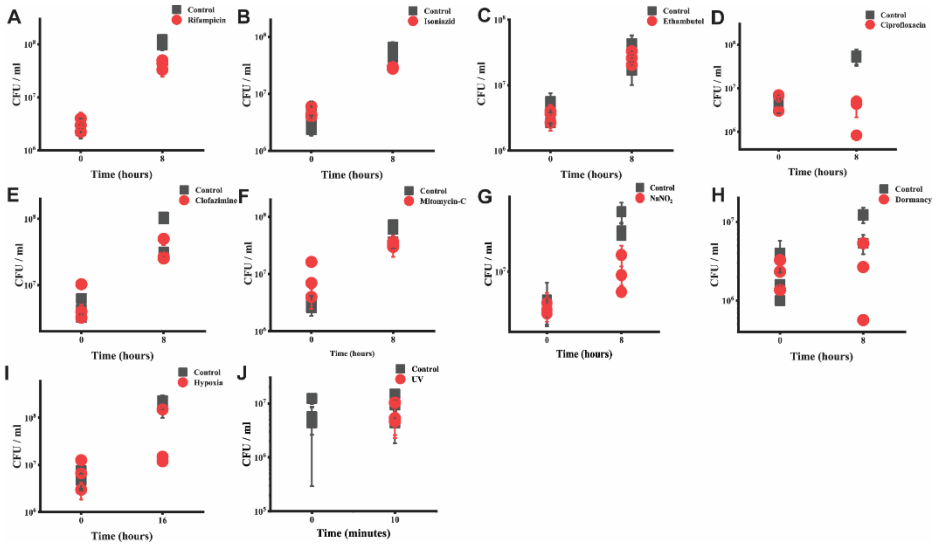

Figure 1: The effect of genotoxic stress treatments applied on *Msm* cells. A) Rifampicin, B) Isoniazid, C) Ethambutol, D) Ciprofloxacin, E) Clofazimine, F) Mitomycin-C, G) $NaNO_2$, H) Dormancy, I) Hypoxia, J) UV treatment.

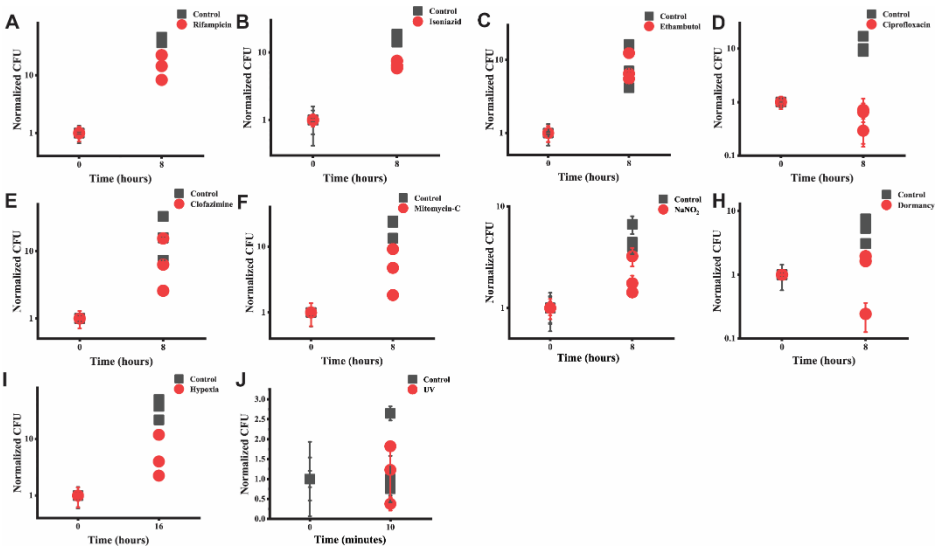

Figure 2: Normalized CFUs of genotoxic stress treatments applied on *Msm* cells. A) Rifampicin, B) Isoniazid, C) Ethambutol, D) Ciprofloxacin, E) Clofazimine, F) Mitomycin-C, G) $NaNO_2$, H) Dormancy, I) Hypoxia, J) UV treatment.

After establishing treatment conditions, we investigated the dNTP pool upon each stress treatment. In most cases, we also determined the average cell size of the treated and non-treated population using microscopy in order to be able to compare cellular dNTP concentrations. The effect of different stresses on the cellular dNTP levels was determined by Éva Viola Surányi and Tamás Trombitás in several years of work and is summarized in **Figure 4**.

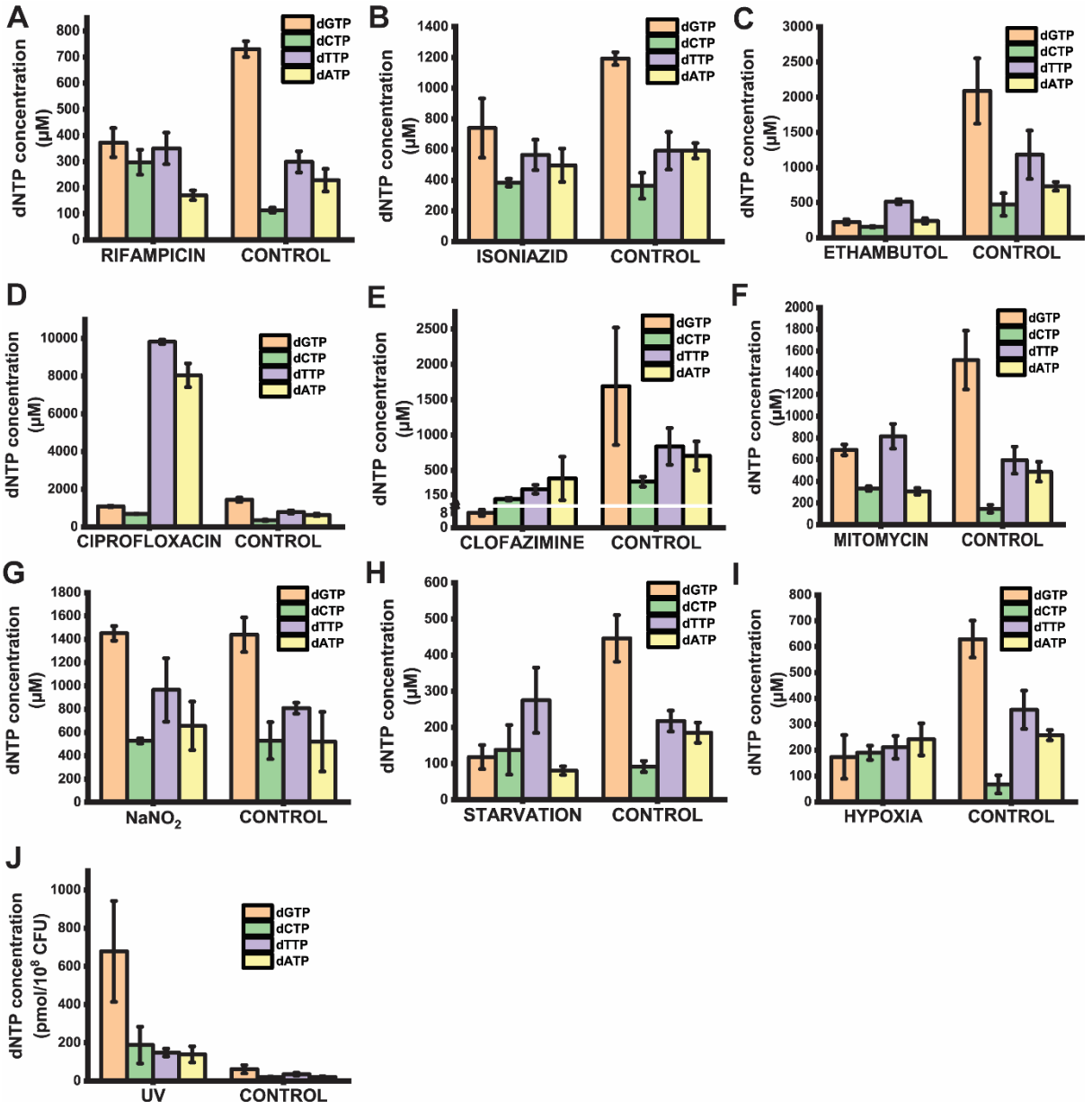

Figure 4: dNTP concentrations upon genotoxic stress treatments applied on *Msm* cells. A) Rifampicin, B) Isoniazid, C) Ethambutol, D) Ciprofloxacin, E) Clofazimine, F) Mitomycin-C, G) $NaNO_2$, H) Dormancy, I) Hypoxia, J) UV treatment.

Interestingly, in most cases, an imbalanced dNTP pool was observed. Not surprisingly, we detected extraordinary changes in the dNTP concentrations upon UV and ciprofloxacin treatments, which underlines their strong genotoxic effect. We observed that a decrease in the otherwise dominating dGTP level seems to be a general stress response. This phenomenon could be observed in case of the rifampicin, isoniazid, ethambutol, ciprofloxacin, clofazimine, mitomycin-C, starvation, and hypoxia treatments (**Figure 4A, B, C, D, E, F, H, I,** respectively). One exception to this phenomenon is the UV treatment where we observed just the opposite (**Figure 4J**). Otherwise, the $NaNO_2$ treatment induces no changes in the dGTP level as it induced no changes at all in any of the dNTP levels (**Figure 4G**). $NaNO_2$ treatment was otherwise effective in inhibiting cell growth (**Figures 2G and 3G**) and thus this

proves that not every stress factor contributes to dNTP changes. We also observed that the levels of dCTP and dTTP are coupled to each other. When the dCTP level was increased, the dTTP level also increased (cf. rifampicin, ciprofloxacin, mitomycin-C, starvation and UV treatments, **Figure 4A, D, F, H, J,** respectively), while the decreased level of dCTP coincided with the decreased level of dTTP (cf. ethambutol and clofazimine treatments, **Figure 4C and E,** respectively). When the dCTP level did not change, the dTTP level did not change either (in case of isoniazid and $NaNO_2$ treatments, **Figure 4B and G**, respectively). The reason behind this phenomenon is assuredly the coupled *in vivo* biosynthesis of pyrimidine nucleotides, as dCTP serves as a precursor for dTTP synthesis, while oxidative deamination reaction takes place on dCTP by the Dcd-dut enzyme. The only exception to this trend is the hypoxia treatment (**Figure 4I**), where the dCTP level increased while the dTTP level decreased. Considering that hypoxia treatment normally causes an altered redox potential in the cell and that the dCTP to dTTP conversion includes a reduction step, we concluded that the disturbance of this reduction reaction can lead to the observed dNTP pattern. Interestingly, dTTP is an important nucleotide for cell wall biosynthesis too, since one of the cell wall synthesis enzymes, RmlA, synthesizes dTDP-rhamnose with the use of dTTP. Interestingly, the elevated level of dTTP resulted in an elevated cell size, while the decreased level of dTTP coincided with decreased cell size.

We also identified that dGTP plays a major role in stress response. Literature data also indicate that the level of dGTP plays a key role in mutation generation[12]. It was shown, that decrease in the level of dGTP is not especially mutagenic, however, its increase causes high mutagenicity of the investigated strains[13,14]. We also observed this phenomenon in the UV treatment as the only treatment causing elevated dGTP level. In this case, high increase in the mutation rate was also observed. Interestingly, literature data also indicate that the decreased level of dGTP contributes to an increased DNA replication fidelity by slowing down replication process which promotes proofreading activity[13]. It is yet to investigate whether this is also the case in a bacterial species in which dGTP is the most abundant dNTP and the GC content of the genome is amongst the highest. Whether this phenomenon contributes to the unusually low basal mutation rate in mycobacteria.

Aim 2: A quantitative model of dNTP metabolism

We created the computational model of the dNTP producing metabolic network of *Mycobacteria* (this set of enzymes is almost identical within the genus) in an attempt to be able to predict the composition of the dNTP pool in various physiological conditions and reveal the mechanistic reasons for the fine-tuned dNTP balance. As dNTP metabolic drugs are being used to treat a variety of diseases, we thought it would be important for antimycobacterial drug design as well. Such comprehensive and quantitative kinetic model does only exist for the folate pathway [15,16] which is a much smaller slice of this pie. We expected that using the known kinetic parameters, the estimated concentrations of the input NDPs and the cellular concentration of the enzymes, our model will be able to reproduce the cellular concentrations of dNTPs measured in Aim 1. Reciprocally, the underlying changes in the dNTP metabolic routes upon stress exposure (Aim 1) could be inferred.

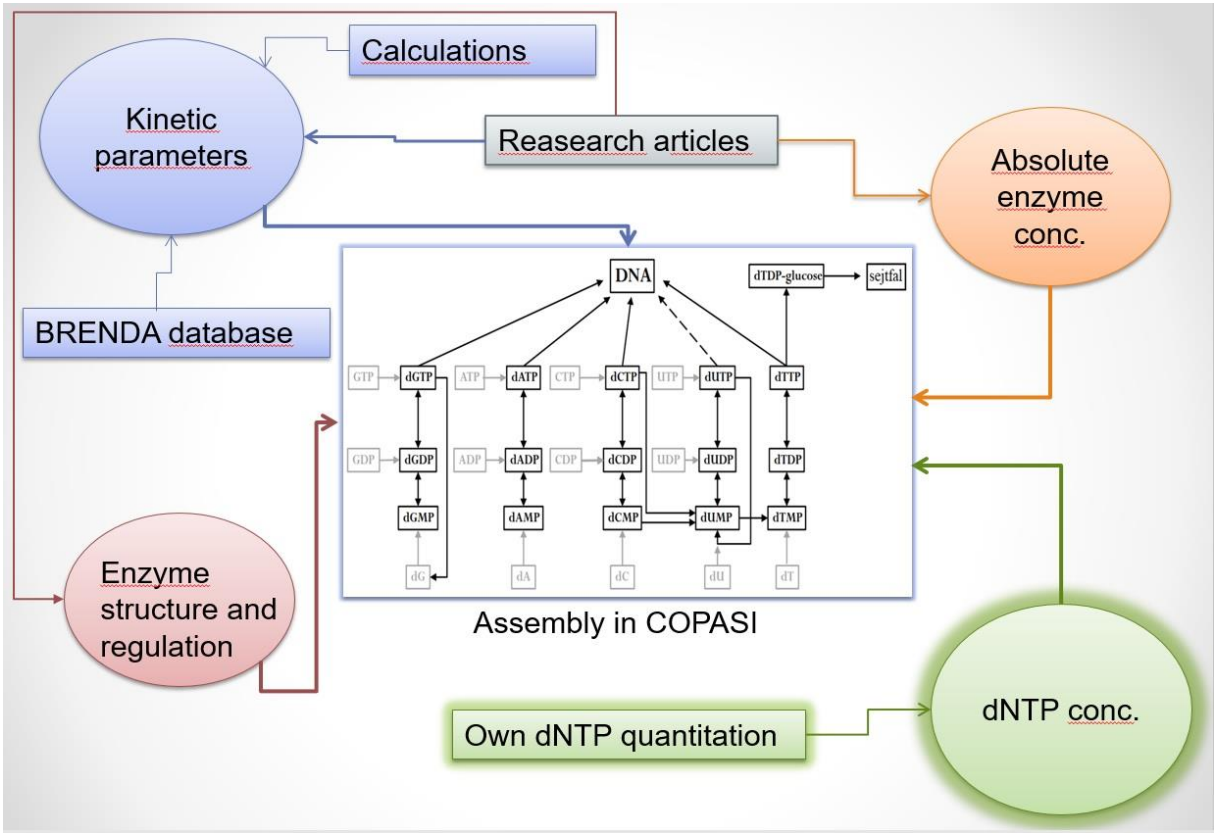

Figure 5: Construction of the kinetic model of the dNTP metabolism of *Mycobacteria*. The figure shows the principles of gaining information that served as input for the kinetic equations in the Copasi software. We chose to break down all processes to basic differential equations which permitted to introduce regulation elements other than already set up in the software. Kinetic parameters were calculated from thermodynamic ones when necessary, imposing thermodynamic constraints and setting binding processes fast enough not to be rate-limiting.

Here again, we run into a major problem: the kinetic model constructed with the available parameters did not reproduce our measured dNTP pools. The regulation of the nucleotide pool balance occurs mainly through the substrate-level allosteric behavior of the enzymes involved in dNTP production (ribonucleotide reductase (RNR) [17] and nucleoside diphosphate kinase (NDK) in the first place). From our growing number of nucleotide pool measurements in various species (**Figure 6**), we realized that i) the nucleotide pool balance is markedly different in the different species, ii) similar pools coincide with similar RNR types acting in those species.

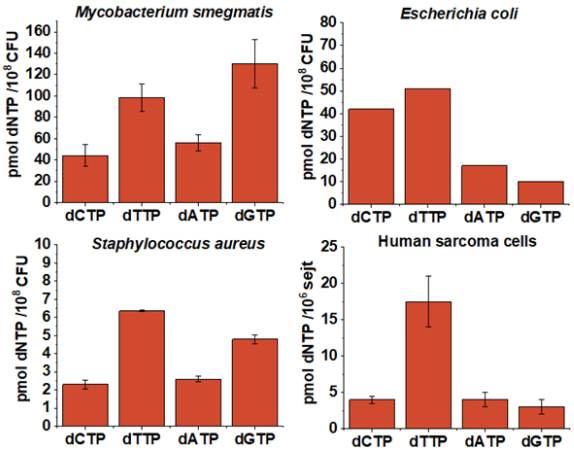

Figure 6: dNTP pool composition in various species

Therefore, we conducted a study to compare various RNR enzymes and their kinetic properties where available to be able to construct this essential part of our dNTP metabolism model. We tried to approach the unknown parameters as much as possible by understanding the structure-function relations of RNR-s. This herein presented example of the RNR shows along what lines we constructed the model, also in the case of the other included enzymes. RNR-s are responsible for the formation of deoxyribonucleotides from ribonucleotides in all domains of life. RNR-s are classified into three main classes of homologues enzymes. The difference between the three classes lies in the subunit composition of RNR complexes, in the active site architecture comprising the radical centrum, and in the regulation of the enzymatic activity [18,19]. *Mtb* and *Msm* encode type Ib, Ic and type II enzymes [20] (**Table 2**).

Ribonucleotide reductase	**Gene name**	**Gene function**	**Gene in *Mtb***	**Gene in *Msm***	
Type I enzyme	*NrdE*	Ribonucleotide reductase large subunit Type Ib	**Rv3051c**	MSMEG2299;	MSMEG 1019
	NrdF	Ribonucleotide reductase small subunit Type Ib	Rv1981c (NrdF1-R2F-1, **Rv3048c (NrdF2-R2F-2)**	MSMEG2313	MSMEG1033
	NrdH	glutaredoxin-like protein (reductant of RNR Ib)	Rv3053c	MSMEG2298	MSMEG1017
	NrdI	Flavodoxin (formation of redox center)	Rv3052c	MSMEG2298 (pseudogene)	MSMEG1018 (pseudogene)

	NrdB	Ribonucleotide reductase small subunit Type Ic	Rv0233c	MSMEG0358	-
Type II enzyme	*NrdZ*	Type II ribonucleotide reductase (homologues with large subunit)	Rv0570c	-	-

Table 2: RNR genes present in the genome of *Mtb* H37Rv and *Msm* mc^{2}155. Data is from Mowa 2009 JB [20],. Essential genes are highlighted in bold.

In our model, we only involved the Type Ib RNR because, according to the literature, the deletion of type Ic and type 2 enzymes did not have an effect under normal or various stress conditions. Of course, both NrdZ and NrdB enzymes may have an impact under yet unknown, special conditions. The basic kinetic mechanism of RNR is shown in **Figure 7A**. Unfortunately, neither for mycobacterial nor for other RNR enzymes are all the parameters determined. Thus, we used a simplified reaction mechanism presented in **Figure 7B**, for which most parameters were measured or could be estimated from at least other species. Although the regulation of RNR-s is relatively conserved, the k*cat* and K*m* values may largely vary between different organisms. We tried to choose an as closely related enzyme as possible. The closest relative proved to be the *Salmonella* RNR for which a broader kinetic investigation was done. Therefore, for CDP and UDP, the RNR specificity pattern and Kd data were taken from *Salmonella*. To construct the model, the following assumptions were made:

1. Two large subunits in the active complex → two substrate binding sites and two specificity sites. Between the two specificity sites cooperativity has been shown for RNRs from different species (Salmonella, murine) → not enough information for modelling therefore it was omitted. S0.5 values were used.

2. Kd parameters for UDP and CDP are the same. Eliasson et al. 1997 [21] stated that they have the same effector requirements. Different specific activity data were taken into consideration.

3. For dATP, CDP both Kd1, Kd3, Kd4 are available. Kd2 can be calculated using the thermodynamic constrain Kd1*Kd3=Kd2*Kd4.

4. For dNTP binding to the large subunit only data at 4°C are available. It is obvious that at higher temperature the Kd increases. In addition, the presence of the small subunit inhibits dNTP binding. Not available dNTP Kd1 values were estimated from the dATP Kd1 value with the assumption that the affinity pattern for the different dNTPs does not alter with a different temperature and with the presence of small subunit. → dTTP, dGTP binding data

5. dGTP-ADP, dTTP-GDP pairs: relatively few data are available, all necessary parameters could not be calculated. Thus *Salmonella* data was combined with *Trypanosoma brucei* data, for which Km was available for every substrate-effector pairs.

6. Kd1 and Kd3 for the GDP-RNR complex was not known, therefore we only used: Kd1*Kd3=Kd2*Kd4=2640

7. For ATP, Kd3 was taken from mycobacterial data. Activated ADP Km (RNR.dATP.ADP) was used from *Salmonella*. ATP is a better activator in *Mycobacterium*. This was considered by using mycobacterial kcat data and by scaling all other kcat-s to this parameter.

We realized that relatively small changes in RNR regulation by various dNTPs may cause a characteristic change in the dNTP pool balance (**cf. Figure 6**). We had no means to obtain more, or more precise parameters for mycobacterial RNR-s. Therefore, after long trials we concluded that a different approach had to be taken. Using the same principles as for the mycobacterial model, we reconstructed the kinetic model of the *E. coli* dNTP metabolic routes for which much more parameters were available and the regulation of RNR and NDK enzymes is best studied. The parameters used to construct this model are presented in the Appendix of this document. The *E. coli* model, indeed, reproduces dNTP pools measured from cell extracts in normal and altered conditions (when dNTP pool is disturbed). Knowing the differences between the enzyme set of *E. coli* and *Mycobacteria*, using a reverse logic, we can now predict the changes in the enzymatic mechanism of RNR necessary to produce a mycobacterial-like dNTP pool. The work presented here were done by Judit Eszter Szabó and Dóra Füzesi.

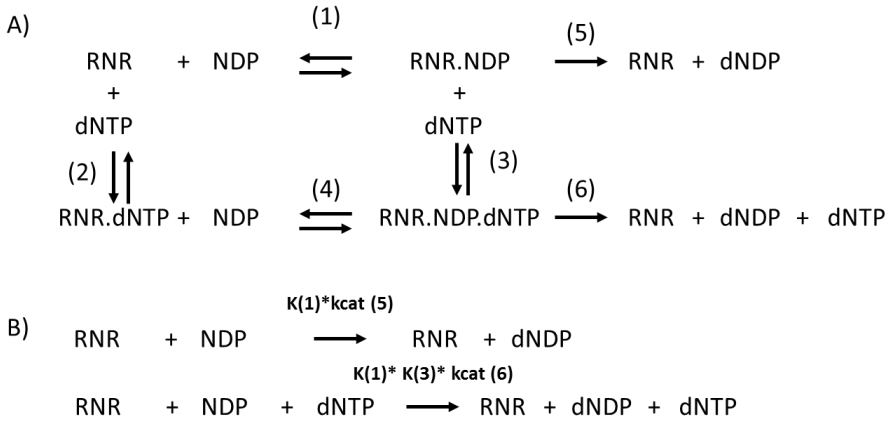

Figure 7: A general RNR reaction mechanism (A) and the simplified model of the reaction mechanism of the mycobacterial RNR (B)

Aim 3: Mutational pattern and DNA repair induction in function of dNTP pool imbalances and expansion

Mutational pattern

We carried out mutation accumulation experiments (led by Rita Hirmondó) under the stress treatment conditions specified in Aim 1. We isolated genomic DNA from the treated samples, subjected the purified DNA to next generation sequencing and analyzed the mutation rate and pattern from whole genome sequencing data. We generated the treated cell lines by streaking single cell colonies from plate to plate. This technique enables that each cell line passes through a single-cell bottleneck. The treatments were carried out for 60 days, which equal approximately 360 generations, considering that treated cells grow slower than non-treated cells. All treatments were carried out from a single cell of a common ancestor, which ancestor was also sent for sequencing. We used 15-16 parallel cell lines for each stress treatments. 60-day experiments repeated several times. We generated non-treated cell

lines for comparison, in this case streaking was carried out for 120 days to accumulate enough mutations for the analysis. The results of our mutation accumulation experiment upon stress treatments are presented in **Figures 8-9**. **Figure 8** shows the cumulative mutation data while **Figure 9** contains a mutational pattern analysis for each treatment. We analyzed the potential manifestation of all mutations as well (genome sequencing data analyzed by Éva Viola Surányi), but the length of this document does not allow a detailed discussion of this aspect. In summary, we could not identify mutational hotspots and not even the "usual suspects", common resistance genes came up. Unexpectedly, most stress treatments did not result in significantly increased mutation rates. Two treatments increased the mutation rate drastically. Not surprisingly, one of them was the UV treatment (**Figure 9K**), which we chose as a 'positive control'. The other mutator strong treatment was the mitomycin-C (**Figure 9G**), an alkylating agent used to mimic alkylating environment of the tuberculosis host. The elevated mutation rate was associated with altered mutation pattern as well: including mostly C:G→T:A transitions and C:G→A:T, C:G→G:C transversions. Note, that all these mutations involve changes of the C:G base pair. A probable reason for this involvement is that cytosine is the most vulnerable base to alkylation on the 5'-carbon atom of its pyrimidine ring. However, with this sequencing technique we could not differentiate the DNA strand that became mutated, it could either be cytosine or guanine. In the other stress treatment cases, smaller changes of the mutation patterns were observed. In connection with that, another interesting phenomenon we found was that the first-line antituberculosis drugs did not increase the mutation rate alone (**Figure 9A-C**). However, in combination and in a hypoxic environment, we observed un unusually high number of mutations present. I will come back to this phenomenon later.

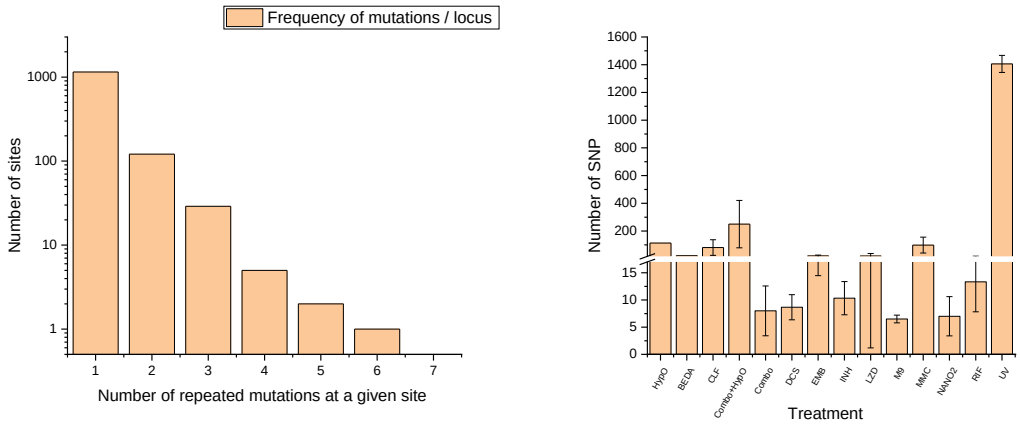

Figure 8: Mutagenic effect of the treatments. A) Frequency of mutations at a given site. The distribution of mutations (cumulated from all treatments) indicates no mutational hotspots. **B**) The number of mutations (single nucleotide polymorphism, SNP) detected upon various treatments. HypO, microanaerob environment; BEDA, bedaquiline; CLF, clofazimin; Combo+HypO, combinations of 1st line drugs+microanaerob environment; Combo, Combination of 1st line drugs (INH+EMB+RIF+Pirazinamide); DCS, D-cycloserine; EMB, ethambutol; INH,Isoniazid; LZD, Linezolid; M9, starvation in M9 broth; MMC,mitomycin-C; NANO, sodium nitrite; RIF, rifampicin

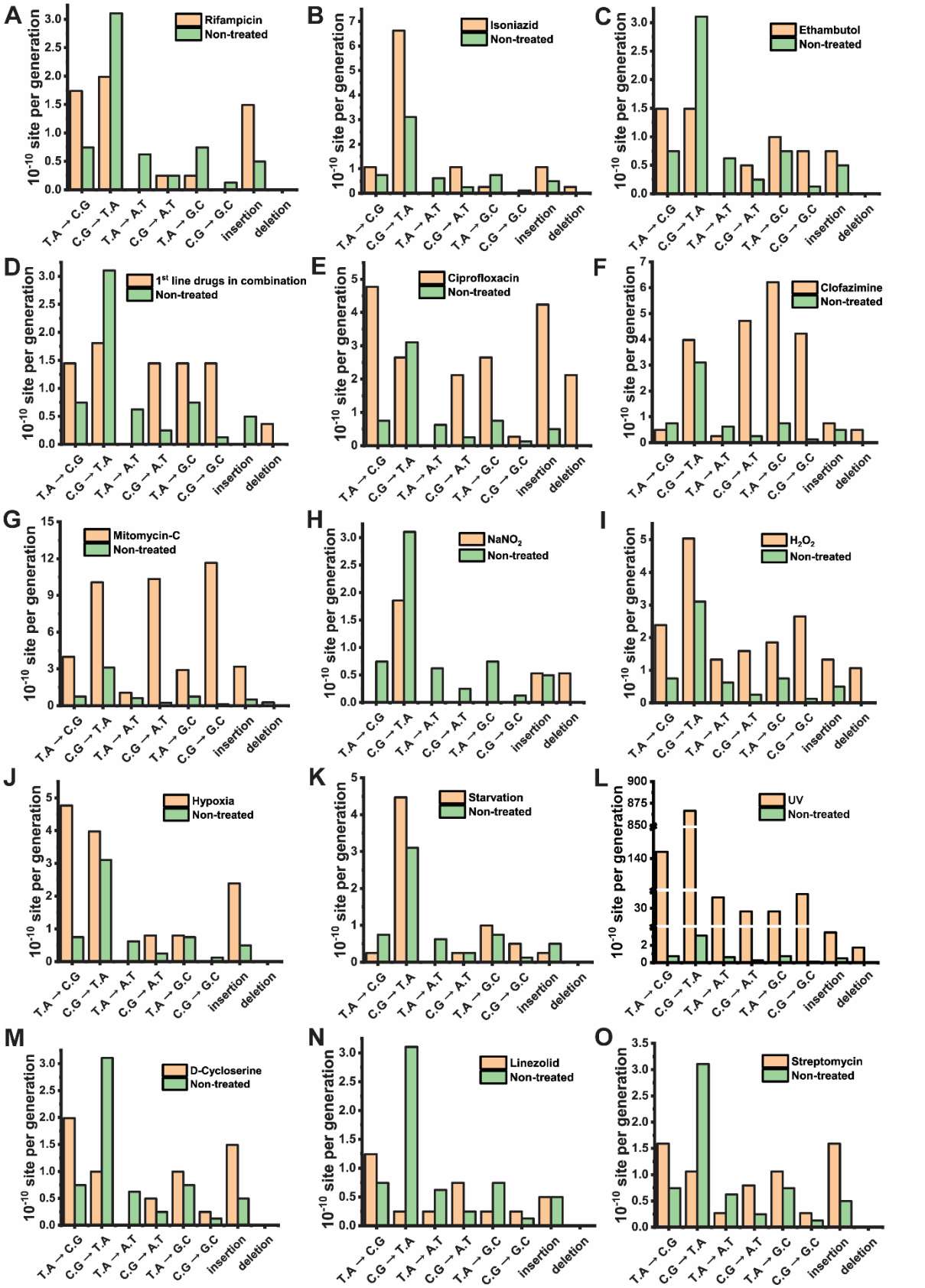

Figure 9: Mutation rate and pattern of *Msm* cells upon genotoxic stress treatments (Éva Viola Surányi)**.** A) Rifampicin, B) Isoniazid, C) Ethambutol, D) First-line drugs in combination, E)

Ciprofloxacin, F) Clofazimine, G) Mitomycin-C, H) $NaNO_2$, I) H_2O_2, J) Hypoxia, K) Starvation, L) UV, M) D-Cycloserine, N) Linezolid, O) Streptomycin.

DNA repair induction

The changes in the expression of DNA repair proteins were investigated upon stress treatments using qPCR. We had to design a whole new qPCR protocol to measure reliable mRNA levels from *Msm* as this technic was not widespread in this organism. RNA isolation was at first difficult from this bacterium surrounded by a think cell wall. The typical reference genes used in other organisms could not be used here. In fact, none of the reference genes alone was adequate, we had to combine 3 of them to provide a stable reference set that did not change with cell culture conditions, growth rate and other influences of the stress treatments. Primer design was a key point, as well, as the GC content of mycobacteria approaches 70 % in the genome. The optimization of the qPCR primers finally resulted in excellent efficiencies shown in **Table 3**. We also faced continuous cross-contamination in the qPCR plates in the Institute no matter how much care we had taken, therefore, we had to move sample preparation to another building, without air conditioning. Due to the significant effort made by Dániel Molnár, PhD student on the project, all issues were resolved, and the data is now ready for publication. The quantification of the expression of the genes investigated upon various stress treatments is concisely presented as heat maps in **Figures 10-12.**

Gene	Primer efficiency (%)
PREVENTIVE REPAIR	
Dcd:dut	98,2
Dut	97,1
MutT1	107
MutT2	86,7
MutT3	92,1
MutT4	87,1
ThyX	94,2
ThyA	92,8
SOS REPAIR	
AdnA	81,6
LexA	105
RecA	90,1
RecX	89,9

Gene	Primer efficiency (%)
GLYCOSYLASES	
AlkA	83,5
Mpg	89,6
MutM1	93,0
MutY	86,4
Nei1	99,7
Nei2	92,1
Ogt	92,6
TagA	91,4
UdgB	97,1
UdgX	91,8
Ung	89,2

Gene	Primer efficiency (%)
ENDONUCLEASES	
End	83,0
NucS	99,7
XthA	80,7
DNA SYNTESIS	
DinB1	83,2
DinB2	81,2
DNAE2	87,7
DNA lig.	91,1
PolA	83,9
PEROXIDASES	
AhpC	103
KatG1	96

Gene	Primer efficiency (%)
NUCL. EXCISION	
Mfd	89,0
UvrA	94,6
UvrB	96,6
UvrC	88,1
UvrD	86,3
REFERENCE GENES	
Ffh	86,2
SigA	87,7

Table 3: Efficiency of the optimized primers used to quantify mRNA in whole RNA *Msm* extracts. Efficiency tests were run using quantified genomic DNA.

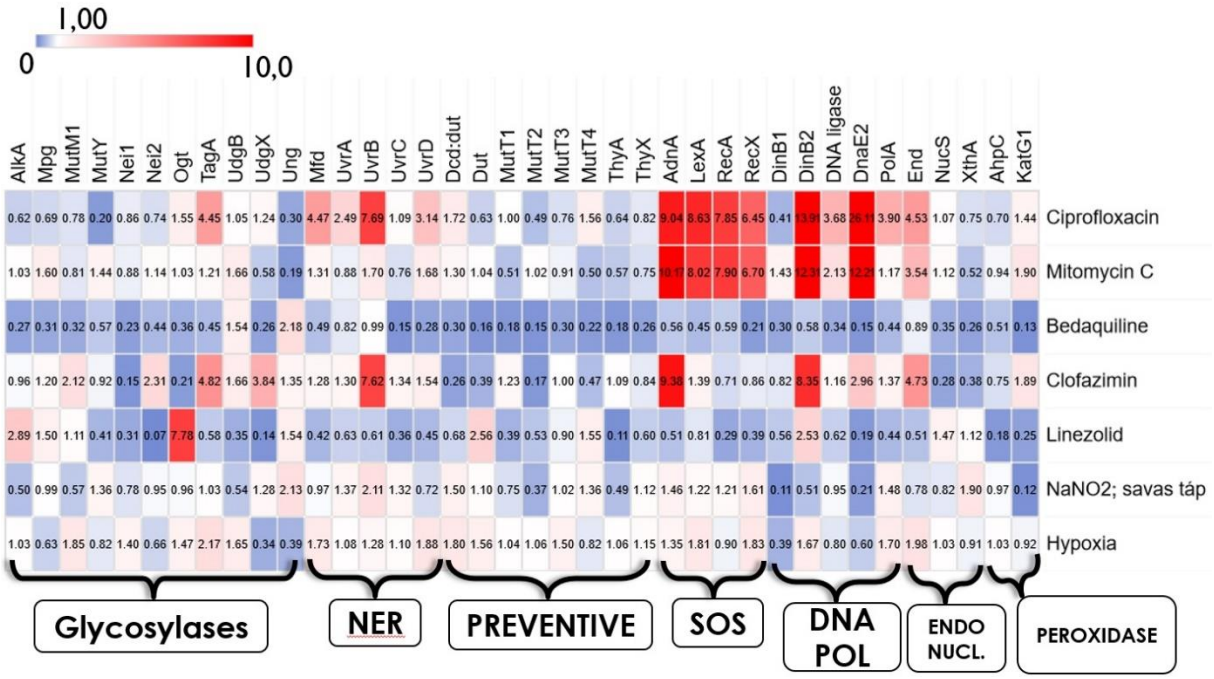

Figure 10: Expression patterns of DNA repair genes in *Msm* upon treatment with second line antituberculotics and environmental stresses. Fold changes in the expression levels compared to the non-treated sample are shown in the squares.

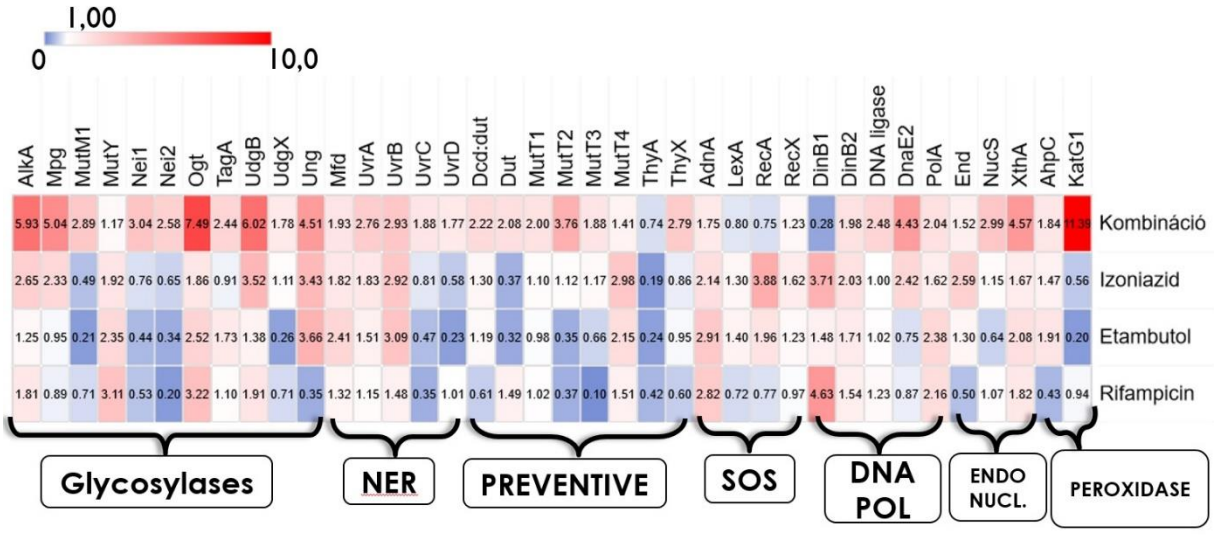

Figure 11: Expression patterns of DNA repair genes in *Msm* upon treatment with first line antituberculotics alone or in combination. Fold changes in the expression levels compared to the non-treated sample are shown in the squares.

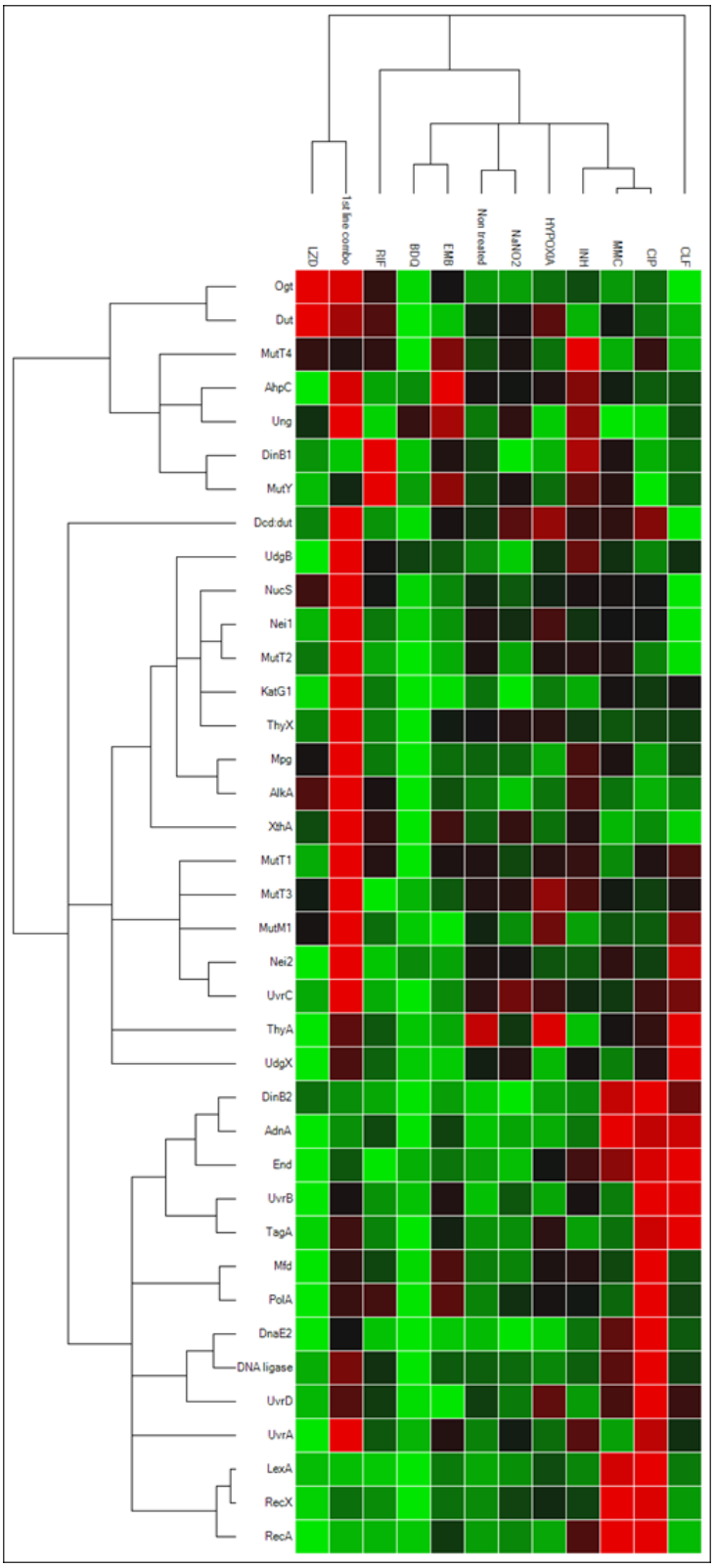

Figure 12: Clusterogram of the expression patterns of DNA repair genes in *Msm* upon all treatments carried out. Treatments are shown in columns and investigated genes in rows (same abbreviations as in Figs. 8-9). The lighter the red, the higher the gene expression level within a column, and conversely, the lighter the green, the more decreased the expression level. Black means no changes compared to the non-treated sample. This representation shows that stress factors which cause similar damage, induce similar cell response in terms of the activation of the DNA-repair machinery. Treatments that induce a general decrease in cell proliferation without targeted DNA damage, e.g. hypoxia and nitrosative stress, have mild effect on the DNA repair system. The treatment with the two agents known to induce double strand DNA breaks, ciprofloxacin and mitomycin C, have almost identical patterns. The SOS response seems to have a crucial role in repairing these lesions.

Papers in preparation

In the previous sections, I have tried to show part of the data we had collected to fulfil our aims. This set of data carries a wealth of information. We try to optimize the publication plan to produce at least 2 more high-profile papers (IF > 10, 1-2 in the list below), and several others in less prestigious journals (IF = 4-5, still D1) of the remaining data this year.

1. The molecular mechanism of the mutator effect of the first-line antituberculosis combination therapy

The first-line treatment of tuberculosis is a combination therapy using 4 drugs: rifampicin, isoniazid, ethambutol and pyrazinamide. At some point of the study, we omitted the latter from our investigations as it had no effect on *Msm*. It was reported to be pumped out of the cell[22]. These drugs are used in combination for two reasons: 1) to reach the pathogen at various sites in the body and 2) to avoid the rapid emergence of drug resistance. When analysing the results, we noticed that these drugs used separately had little effect on the investigated parameters, while their application in combination and under hypoxic environment resulted in a mutator effect and characteristic changes in the dNTP pool and DNA repair gene expression pattern. **Figure 11** shows that the combination treatment turned on the KatG peroxidase that is responsible to convert the isoniazid prodrug to its active form, as well as DNA glycosylases responsible for base excision DNA repair (removal of damaged or incorrect bases from the genome). At the same time, a large number of mutations appeared in the sample of the first-line drugs used in combination. However, these mutations appeared at low frequency in the sequenced samples supposed to be derived from single colonies. We investigated whether this phenomenon could be an artefact of sequencing, but we did not find any evidence for this. We found that the distribution of mutations along the genome is different in hypoxic treatment better mimicking the real-life situation in a treated patient. The combination of first-line drugs and hypoxia resulted in mutations appearing spatially close to each other (**Figure 13**) which indicates a specific mechanism responsible for the appearance of these mutations. This phenomenon coincides with the upregulation of the error-prone polymerase DnaE2 (**Figure 11**) which was previously shown to contribute to the emergence of drug resistance in *Mtb*[23]. This observation indicates a mechanism whereby DNA damage upon drug treatment induces long-patch DNA repair with the action of the error-prone DnaE2 polymerase.

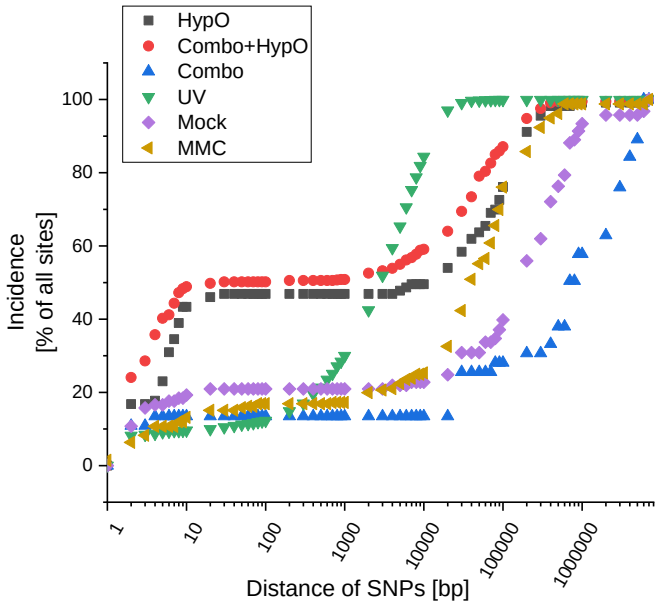

Figure 13: The incidence of mutations along the genome. HypO, microanaerob environment; Combo+HypO, combinations of 1st line drugs+microanaerob environment; Combo, Combination of 1st line drugs (INH+EMB+RIF+Pirazinamide); MMC,mitomycin-C; MOCK, non-treated reference

We propose that many of the observed low frequency mutations arose when cells were relieved from stress treatment, i.e. it is the result of the final cell growth of single colonies in liquid media for the purpose of DNA preparation. In this case, we did not detect these mutations in our analysis as single colony mutations. We hypothesize that the multiplication of the chromosome and the accumulation of mutations occur without cell division during stress treatment. Then, once colonies are grown in liquid media, cell division occurs and results in the manifestation of genetic variety from a seemingly uniform single cell colony. We attribute great importance to this phenomenon as having major role in antibiotic resistance development upon the interruption of drug treatments. When host treatment is interrupted and bacteria are released from antibiotics, the remaining bacterial population may potentially have higher mutation rate which gives rise to the generation of antibiotic resistance genes.

There seems to be a discrepancy between our molecular biology results and the clinical observation in that the first-line drugs applied together are more, or just the opposite, less likely to induce drug resistance than the same drugs applied separately. We propose that this seeming contradiction can be resolved by the distinction of phenotypic versus genotypic drug resistance. Phenotypic resistance means that the susceptibility to antibiotics decreases without any genetic alterations e.g. by changes in the metabolic state of the organism, or by the overexpression of efflux pumps that lower the intracellular concentration of the drug. These phenotypic changes may quickly occur. On the other hand, genotypic resistance arises by mutations and even under the pressure of genotoxic stress, it takes more time. However, once derived, resistance is stable, and resistant strains prevail. We propose that our observations upon the combination treatment belong to the latter phenomenon, while the rapid clinical emergence of resistance to individual drugs might arise by the phenotypic mechanism.

2. The kinetic model of the *E. coli* dNTP metabolism

This manuscript presents the largest quantitative metabolic model published so far that integrates measured kinetic parameters, measured enzyme and metabolite concentrations and the knowledge on enzymatic mechanisms. All parameters used to construct the model are shown in the Appendix (created by Dóra Füzesi). This model can predict the effect of changes in any of these parameters on the whole system. We built in DNA synthesis and cell wall synthesis as outputs of dNTP production so that dNTP changes can be followed in function of the cell cycle. Vice versa, the effect of a drug targeting dNTP metabolism can be predicted on cell growth.

3. The regulation of ribonucleotide reductase defines the dNTP pool balance

As mentioned earlier, we did not have enough original parameters to reconstruct the mycobacterial dNTP metabolic model due to the fact that the kinetic parameters for mycobacteria could not be replaced even by parameters from organisms expressing RNRs of the same enzyme subfamily. We measured the dNTP pools of several different organisms and several others are published. Using these data and the information on the type of RNRs in these organisms we can relate the two phenomena and predict, based on genomic information, the dNTP constitution of an organism.

4. The effect of environmental stress on the dNTP pool and DNA repair in *Mycobacterium smegmatis*

Surprisingly, some of these stresses resulted in only subtle changes in the mutation rate or in the dNTP pool e.g. starvation or $NaNO_2$. I explained in detail the mechanism of mutation induction by oxidative stress applied in the form of H_2O_2 in the report of last year.

5. The effect of alkylating agents on the dNTP pool and DNA repair in *Mycobacterium smegmatis*

We find these findings worth publishing in a separate paper as alkylating agents are being heavily used in research and macrophages use alkylation as a defense against intracellular pathogens. These drugs showed large and characteristic changes in the mutational pattern and in DNA repair activation while dNTP pool changes were not uniform. A molecular mechanism of action of inducing mutations can be inferred which we think is of interest for the scientific community.

References

(1) Szabó, J. E., Surányi, É. V., Mébold, B., Trombitás, T., Cserepes, M., and Tóth, J. (2020) A user-friendly, high-throughput tool for the precise quantitation of deoxyribonucleoside triphosphates from biological samples. *Nucleic Acids Res. 1*, 1–17.

(2) Surányi, É. V., Hírmondó, R., Nyíri, K., Tarjányi, S., Kőhegyi, B., Tóth, J., and Vértessy, B. G. (2018) Exploiting a phage-bacterium interaction system as a molecular switch to decipher macromolecular interactions in the living cell. *Viruses 10*.

(3) Lopata, A., Jójárt, B., Surányi, É. V., Takács, E., Bezúr, L., Leveles, I., Bendes, Á., Viskolcz, B., Vértessy, B. G., and Tóth, J. (2019) Beyond chelation: EDTA tightly binds taq DNA polymerase, MutT and dUTPase and directly inhibits dNTPase activity. *Biomolecules 9*.

(4) McGrath, M., Gey van Pittius, N. C., van Helden, P. D., Warren, R. M., and Warner, D. F. (2014) Mutation rate and the emergence of drug resistance in Mycobacterium tuberculosis. *J. Antimicrob. Chemother. 69*, 292–302.

(5) Ford, C. B., Lin, P. L., Chase, M. R., Shah, R. R., Iartchouk, O., Galagan, J., Mohaideen, N., Ioerger, T. R., Sacchettini, J. C., Lipsitch, M., Flynn, J. L., and Fortune, S. M. (2011) Use of whole genome sequencing to estimate the mutation rate of Mycobacterium tuberculosis during latent infection. *Nat. Genet. 43*, 482–6.

(6) Sun, G., Luo, T., Yang, C., Dong, X., Li, J., Zhu, Y., Zheng, H., Tian, W., Wang, S., Barry, C. E., Mei, J., and Gao, Q. (2012) Dynamic population changes in Mycobacterium tuberculosis during acquisition and fixation of drug resistance in patients. *J. Infect. Dis. 206*, 1724–33.

(7) Springer, B., Sander, P., Sedlacek, L., Hardt, W.-D., Mizrahi, V., Schär, P., and Böttger, E. C. (2004) Lack of mismatch correction facilitates genome evolution in mycobacteria. *Mol. Microbiol. 53*, 1601–1609.

(8) Mathews, C. K. (2014) Deoxyribonucleotides as genetic and metabolic regulators. *FASEB J.* 1–9.

(9) WHO. (2019) Global Tuberculosis Report.

(10) Klopper, M., Warren, R. M., Hayes, C., Gey van Pittius, N. C., Streicher, E. M., Müller, B., Sirgel, F. A., Chabula-Nxiweni, M., Hoosain, E., Coetzee, G., David van Helden, P., Victor, T. C., and Trollip, A. P. (2013) Emergence and spread of extensively and totally drug-resistant tuberculosis, South Africa. *Emerg. Infect. Dis. 19*, 449–55.

(11) Udwadia, Z. F., Amale, R. A., Ajbani, K. K., and Rodrigues, C. (2012) Totally Drug-Resistant Tuberculosis in India. *Clin. Infect. Dis. 54*, 579–581.

(12) Ahluwalia, D., and Schaaper, R. M. (2013) Hypermutability and error catastrophe due to defects in ribonucleotide reductase. *Proc. Natl. Acad. Sci. U. S. A. 110*, 18596–601.

(13) Schmidt, T. T., Sharma, S., Reyes, G. X., Gries, K., Gross, M., Zhao, B., Yuan, J.-H., Wade, R., Chabes, A., and Hombauer, H. (2019) A genetic screen pinpoints ribonucleotide reductase residues that sustain dNTP homeostasis and specifies a highly mutagenic type of dNTP imbalance. *Nucleic Acids Res. 47*, 237–252.

(14) Martomo, S. A., and Mathews, C. K. (2002) Effects of biological DNA precursor pool asymmetry upon accuracy of DNA replication in vitro. *Mutat. Res. 499*, 197–211.

(15) Nijhout, H. F., Reed, M. C., Budu, P., and Ulrich, C. M. (2004) A mathematical model of the folate cycle: New insights into folate homeostasis. *J. Biol. Chem. 279*, 55008–55016.

(16) Leduc, D., Escartin, F., Nijhout, H. F., Reed, M. C., Liebl, U., Skouloubris, S., and Myllykallio, H. (2007) Flavin-dependent thymidylate synthase ThyX activity: Implications for the folate cycle in bacteria. *J. Bacteriol. 189*, 8537–8545.

(17) Nordlund, P., and Reichard, P. (2006) Ribonucleotide reductases. *Annu. Rev. Biochem. 75*, 681–706.

(18) Torrents, E. (2014) Ribonucleotide reductases: essential enzymes for bacterial life. *Front. Cell. Infect. Microbiol. 4*, 52.

(19) Reichard, P. (2002) Ribonucleotide reductases: the evolution of allosteric regulation. *Arch. Biochem. Biophys. 397*, 149–55.

(20) Mowa, M. B., Warner, D. F., Kaplan, G., Kana, B. D., and Mizrahi, V. (2009) Function and regulation of class I ribonucleotide reductase-encoding genes in mycobacteria. *J. Bacteriol. 191*, 985–95.

(21) Eliasson, R., Pontis, E., Jordan, A., and Reichard, P. (1996) Allosteric regulation of the third ribonucleotide reductase (NrdEF enzyme) from enterobacteriaceae. *J. Biol. Chem. 271*, 26582–26587.

(22) Zhang, Y., Scorpio, A., Nikaido, H., and Sun, Z. (1999) Role of acid pH and deficient efflux of pyrazinoic acid in unique susceptibility of Mycobacterium tuberculosis to pyrazinamide. *J. Bacteriol. 181*, 2044–2049.

(23) Boshoff, H. I. M., Reed, M. B., Barry Iii, C. E., and Mizrahi, V. (2003) DnaE2 Polymerase Contributes to In Vivo Survival and the Emergence of Drug Resistance in Mycobacterium tuberculosis. *Cell 113*, 183–193.

Appendix

Enzyme parameters used to construct the kinetic model of the *E. coli* dNTP metabolic network

enzyme	catalysed reaction	reaction step	equation	parameter name	parameter value	parameter dimension	from literature or calculated	note	reference
adenylate kinase (adk)	dAMP phosphorylation	dAMP binding	AMK + dAMP = AMK.dAMP	Michaelis constant (Km)	1,7	mM	literature	-	(Holmes és Singer, 1973)
adenylate kinase (adk)	(d)AMP phosphorylation	ATP binding	AMK + ATP = AMK.ATP	Michaelis constant (Km)	0,38	mM	literature	-	(Holmes és Singer, 1973)
adenylate kinase (adk)	dAMP phosphorylation	dAMP phosphorylation by ATP	AMK.ADP.dADP = AMK.ATP.dAMP	Vmax	44600	mol substrate/ min/ mol enzyme	literature	-	(Holmes és Singer, 1973)
adenylate kinase (adk)	dAMP phosphorylation	dAMP phosphorylation by ATP reverse	AMK.ADP.dADP = AMK.ATP.dAMP	kcat	600	1/s	calculated	Based on (Bernard, 2000), calculated using reaction K'	-
adenylate kinase (adk)	dAMP phosphorylation	dADP binding	AMK + dADP = AMK.dADP	Michaelis constant (Km)	0,92	mM	literature	-	(Bernard *és mtsai.*, 2000)
adenylate kinase (adk)	(d)AMP phosphorylation	ADP binding	AMK + ADP = AMK.ADP	Michaelis constant (Km)	0,09	mM	literature	-	(Holmes és Singer, 1973)
adenylate kinase (adk)	(d)AMP phosphorylation	dATP binding	AMK + dATP = AMK.dATP	Michaelis constant (Km)	0,25	mM	literature	-	(Holmes és Singer, 1973)
adenylate kinase (adk)	(d)AMP phosphorylation	dAMP phosphorylation by dATP	AMK.dADP.dADP = AMK.dATP.dAMP	Vmax	44600	mol substrate/ min/ mol enzyme	calculated	dAMP-ATP data used from (Bernard, 2000)	-
adenylate kinase (adk)	(d)AMP phosphorylation	dAMP phosphorylation by dATP reverse	AMK.dADP.dADP = AMK.dATP.dAMP	kcat	670	1/s	calculated	Based on (Bernard, 2000), calculated using reaction K'	-
adenylate kinase (adk)	(d)AMP phosphorylation	AMP binding	AMK + AMP = AMK.AMP	Michaelis constant (Km)	0,14	mM	literature	-	(Holmes és Singer, 1973)

enzyme	catalysed reaction	reaction step	equation	parameter name	parameter value	parameter dimension	from literature or calculated	note	reference
adenylate kinase (adk)	(d)AMP phosphorylation	AMP phosphorylation by ATP	AMK.ADP.ADP = AMK.ATP.AMP	Vmax	16500	mol substrate/ min/ mol enzyme	literature	-	(Holmes és Singer, 1973)
adenylate kinase (adk)	(d)AMP phosphorylation	AMP phosphorylation by ATP reverse	AMK.ADP.ADP = AMK.ATP.AMP	Vmax	15800	mol substrate/ min/ mol enzyme	literature	-	(Holmes és Singer, 1973)
adenylate kinase (adk)	dATP production	dADP phosphorylation	AMK.ADP.dADP = AMK.AMP.dATP	kcat	6	1/s	literature	-	(Bernard *és mtsai.*, 2000)
adenylate kinase (adk)		dADP phosphorylation reverse	AMK.ADP.dADP = AMK.AMP.dATP	kcat	7	1/s	calculated	Based on (Bernard, 2000), calculated using reaction K'	-
adenylate kinase (adk)	dGTP production	dGDP binding	AMK + dGDP = AMK.dGDP	Michaelis constant (Km)	0,497	µM	literature	-	(Bernard *és mtsai.*, 2000)
adenylate kinase (adk)	dGTP production	dGTP phosphorylation by ADP	AMK.ADP.dGDP = AMK.AMP.dGTP	kcat	7	1/s	calculated	Based on (Bernard, 2000), calculated using reaction K'	-
adenylate kinase (adk)	dGTP production	dGTP phosphorylation by ADP reverse	AMK.ADP.dGDP = AMK.AMP.dGTP	kcat	4,1	1/s	literature	-	(Bernard *és mtsai.*, 2000)
adenylate kinase (adk)	dGTP production	dGTP binding	AMK + dGTP = AMK.dGTP	Michaelis constant (Km)	3570	µM	calculated	calculated from other NTP and NDP affinities	-
adenylate kinase (adk)	dGTP production	dGTP phosphorylation by dADP	AMK.dADP.dGDP = AMK.dAMP.dGTP	kcat	9	1/s	calculated	Based on (Bernard, 2000), calculated using reaction K'	-
adenylate kinase (adk)	dGTP production	dGTP phosphorylation by dADP reverse	AMK.dADP.dGDP = AMK.dAMP.dGTP	kcat	4	1/s	calculated	(Bernard, 2000), dGDP-ADP data used	(Bernard *és mtsai.*, 2000)
adenylate kinase (adk)	dCTP production	dCDP binding	AMK + dCDP = AMK.dCDP	Michaelis constant (Km)	2180	µM	literature	-	(Bernard *és mtsai.*, 2000)
adenylate kinase (adk)	dCTP production	dCDP phosphorylation by ADP	AMK.ADP.dCDP = AMK.AMP.dCTP	kcat	1	1/s	calculated	Based on (Bernard, 2000), calculated using reaction K'	-

enzyme	catalysed reaction	reaction step	equation	parameter name	parameter value	parameter dimension	from literature or calculated	note	reference
adenylate kinase (adk)	dCTP production	dCDP phosphorylation by ADP reverse	AMK.ADP.dCDP = AMK.AMP.dCTP	kcat	5	1/s	literature	-	(Bernard *és mtsai.*, 2000)
adenylate kinase (adk)	dCTP production	dCTP binding	AMK + dCTP = AMK.dCTP	Michaelis constant (Km)	1250	µM	calculated	calculated from other NTP and NDP affinities	-
adenylate kinase (adk)	dCTP production	dCDP phosphorylation by dADP	AMK.dADP.dCDP = AMK.dAMP.dCTP	kcat	1	1/s	calculated	Based on (Bernard, 2000), calculated using reaction K'	-
adenylate kinase (adk)	dCTP production	dCDP phosphorylation by dADP reverse	AMK.dADP.dCDP = AMK.dAMP.dCTP	kcat	5	1/s	calculated	(Bernard, 2000), dCDP-ADP data used	-
adenylate kinase (adk)	dTTP production	dTDP binding	AMK + dTDP = AMK.dTDP	Michaelis constant (Km)	458	µM	literature	-	(Bernard *és mtsai.*, 2000)
adenylate kinase (adk)	dTTP production	dTDP phosphorylation by ADP	AMK.ADP.dTDP = AMK.AMP.dTTP	kcat	3	1/s	calculated	Based on (Bernard, 2000), calculated using reaction K'	-
adenylate kinase (adk)	dTTP production	dTDP phosphorylation by ADP reverse	AMK.ADP.dTDP = AMK.AMP.dTTP	kcat	4	1/s	literature	-	(Bernard *és mtsai.*, 2000)
adenylate kinase (adk)	dTTP production	dTTP binding	AMK.dTTP = AMK + dTTP	Michaelis constant (Km)	1562	µM	calculated	calculated from other NTP and NDP affinities	-
adenylate kinase (adk)	dTTP production	dTDP phosphorylation by dADP	AMK.dADP.dTDP = AMK.dAMP.dTTP	kcat	4	1/s	calculated	Based on (Bernard, 2000), calculated using reaction K'	-
adenylate kinase (adk)	dTTP production	dTDP phosphorylation by dADP reverse	AMK.dADP.dTDP = AMK.dAMP.dTTP	kcat	4	1/s	calculated	(Bernard, 2000), dTDP-ADP data used	-
guanylate kinase (gmk)	(d)GDP phosphorylation	ATP binding	GMK + ATP = GMK.ATP	Michaelis constant (Km)	63	µM	literature	-	(Hible *és mtsai.*, 2006)
guanylate kinase (gmk)	(d)GDP phosphorylation	dGMP binding	GMK + dGMP = GMK.dGMP	Michaelis constant (Km)	0,185	µM	calculated	calculated from literature data (5x the Km of GMP)	(Oeschger, 1978)

enzyme	catalysed reaction	reaction step	equation	parameter name	parameter value	parameter dimension	from literature or calculated	note	reference
guanylate kinase (gmk)	(d)GDP phosphorylation	dGMP phosphorylation by ATP	GMK.dGMP.ATP = GMK.dGDP.ADP	kcat	188	1/s	calculated	Based on (Hibble, 2006), calculated using reaction K'	-
guanylate kinase (gmk)	(d)GDP phosphorylation	dGDP reverse reaction by ADP	GMK.dGMP.ATP = GMK.dGDP.ADP	kcat	55	1/s	calculated	Based on (Hibble, 2006), calculated using reaction K'	-
guanylate kinase (gmk)	(d)GDP phosphorylation	dGDP binding	GMK + dGDP = GMK.dGDP	Michaelis constant (Km)	0,17	µM	calculated	calculated from other NTP and NDP affinities	-
guanylate kinase (gmk)	(d)GDP phosphorylation	ADP binding	GMK + ADP = GMK.ADP	Michaelis constant (Km)	23	µM	literature	-	(Hible *és mtsai.*, 2006)
guanylate kinase (gmk)	(d)GDP phosphorylation	dATP binding	GMK + dATP = GMK.dATP	Michaelis constant (Km)	0,144	µM	calculated	calculated from other NTP and NDP affinities	-
guanylate kinase (gmk)	(d)GDP phosphorylation	dGMP phosphorylation by dATP	GMK.dGMP.dATP = GMK.dGDP.dADP	kcat	188	1/s	calculated	Based on (Hibble, 2006), calculated using reaction K'	-
guanylate kinase (gmk)	(d)GDP phosphorylation	dGDP reverse reaction by dADP	GMK.dGMP.dATP = GMK.dGDP.dADP	kcat	55	1/s	calculated	Based on (Hibble, 2006), calculated using reaction K'	-
guanylate kinase (gmk)	(d)GDP phosphorylation	dADP binding	GMK + dADP = GMK.dADP	Michaelis constant (Km)	53	µM	calculated	calculated from other NTP and NDP affinities	-
guanylate kinase (gmk)	(d)GDP phosphorylation	GMP binding	GMK + GMP = GMK.GMP	Michaelis constant (Km)	37	µM	literature	-	(Hible *és mtsai.*, 2006)
guanylate kinase (gmk)	(d)GDP phosphorylation	GMP phosphorylation by ATP	GMK.GMP.ATP = GMK.GDP.ADP	kcat	188	1/s	calculated	-	(Hible *és mtsai.*, 2006)
guanylate kinase (gmk)	(d)GDP phosphorylation	GDP reverse reaction by ATP	GMK.GMP.ATP = GMK.GDP.ADP	kcat	55	1/s	literature	-	(Hible *és mtsai.*, 2006)
guanylate kinase (gmk)	(d)GDP phosphorylation	GMP phosphorylation by dATP	GMK.GMP.dATP = GMK.GDP.dADP	kcat	188	1/s	calculated	Based on (Hibble, 2006), calculated using reaction K'	-
guanylate kinase (gmk)	(d)GDP phosphorylation	GDP reverse reaction by dATP	GMK.GMP.dATP = GMK.GDP.dADP	kcat	55	1/s	calculated	Based on (Hibble, 2006), calculated using reaction K'	-

enzyme	catalysed reaction	reaction step	equation	parameter name	parameter value	parameter dimension	from literature or calculated	note	reference
guanylate kinase (gmk)	(d)GDP phosphorylation	GDP binding	GMK + GDP = GMK.GDP	Michaelis constant (Km)	33	µM	literature	-	(Hible *és mtsai.*, 2006)
cytidylate kinase (cmk)	(d)CMP phosphorylation	ATP binding	CMK + ATP = CMK.ATP	Michaelis constant (Km)	0,038	mM	literature		(Bucurenci *és mtsai.*, 1996)
cytidylate kinase (cmk)	dCMP phosphorylation	dCMP binding	CMK + dCMP = CMK.dCMP	Michaelis constant (Km)	0,094	mM	literature		(Bucurenci *és mtsai.*, 1996)
cytidylate kinase (cmk)	dCMP phosphorylation	dCMP phosphorylation by ATP	CMK.dCMP.ATP = CMK.dCDP.ADP	specific activity	226	µmol/ mg*min	literature	average of measured parameters from literature	
cytidylate kinase (cmk)	dCMP phosphorylation by dATP	dCMP phosphorylation by dATP	CMK.dCMP.dATP = CMK.dCDP.dADP	specific activity	219	µmol/ mg*min	literature	average of measured parameters from literature	
cytidylate kinase (cmk)	dCMP phosphorylation by ATP	dCDP reverse reaction by ADP	CMK.dCMP.ATP = CMK.dCDP.ADP	kcat	202	1/s	calculated	calculated from K' calculated for reaction	-
cytidylate kinase (cmk)	dCMP phosphorylation by dATP	dCDP reverse reaction by dADP	CMK.dCMP.dATP = CMK.dCDP.dADP	kcat	222	1/s	calculated	calculated from K' calculated for reaction	-
cytidylate kinase (cmk)	dCMP phosphorylation by ATP	dCDP binding	CMK + dCDP = CMK.dCDP	Michaelis constant (Km)	0,14	mM	calculated	calculated from other Km parameters	-
cytidylate kinase (cmk)	(d)CMP phosphorylation	ADP binding	CMK + ADP = CMK.ADP	Michaelis constant (Km)	0,025	mM	literature		(Bucurenci *és mtsai.*, 1996)
cytidylate kinase (cmk)	(d)CMP phosphorylation	dATP binding	CMK + dATP = CMK.dATP	Michaelis constant (Km)	0,087	mM	literature		(Bucurenci *és mtsai.*, 1996)
cytidylate kinase (cmk)	(d)CMP phosphorylation	dADP binding	CMK + dADP = CMK.dADP	Michaelis constant (Km)	0,067	mM	calculated	calculated from other Km parameters	-
cytidylate kinase (cmk)	CMP phosphorylation	CMP binding	CMK + CMP = CMK.CMP	Michaelis constant (Km)	0,035	mM	literature		(Bucurenci *és mtsai.*, 1996)

enzyme	catalysed reaction	reaction step	equation	parameter name	parameter value	parameter dimension	from literature or calculated	note	reference
cytidylate kinase (cmk)	CMP phosphorylation by ATP	CMP phosphorylation by ATP	CMK.CMP.ATP = CMK.CDP.ADP	specific activity	220	µmol/ mg*min	literature	average of measured parameters from literature	
cytidylate kinase (cmk)	CMP phosphorylation by dATP	CMP phosphorylation by dATP	CMK.CMP.dATP = CMK.CDP.dADP	specific activity	212	µmol/ mg*min	literature	average of measured parameters from literature	
cytidylate kinase (cmk)	CMP phosphorylation by ATP	CDP reverse reaction by ATP	CMK.CMP.ATP = CMK.CDP.ADP	specific activity	410	µmol/ mg*min	literature		(Bucurenci *és mtsai.*, 1996)
cytidylate kinase (cmk)	CMP phosphorylation by dATP	CDP reverse reaction by dATP	CMK.CMP.dATP = CMK.CDP.dADP	kcat	214	1/s	calculated	calculated from K' calculated for reaction	-
cytidylate kinase (cmk)	CMP phosphorylation	CDP binding	CMK + CDP = CMK.CDP	Michaelis constant (Km)	0,052	mM	literature		(Bucurenci *és mtsai.*, 1996)
thymidylate kinase (tmk)	dTMP phosphorylation by ATP	ATP binding	TMK + dATP = TMK.dATP	Michaelis constant (Km)	40	µM	literature		(Munier-Lehmann *és mtsai.*, 2001)
thymidylate kinase (tmk)	dTMP phosphorylation by ATP	dTMP binding	TMK + dTMP = TMK.dTMP	Michaelis constant (Km)	15	µM	literature		(Munier-Lehmann *és mtsai.*, 2001)
thymidylate kinase (tmk)	dTMP phosphorylation by ATP	dTMP phosphorylation by ATP	TMK.dTMP.ATP = TMK.dTDP.ADP	kcat	10,5	1/s	literature		(Munier-Lehmann *és mtsai.*, 2001)
thymidylate kinase (tmk)	dTMP phosphorylation by ATP	dTMP phosphorylation by ATP reverse	TMK.dTMP.ATP = TMK.dTDP.ADP	kcat	5,4	1/s	calculated	Calculated from K' and Km data	-
thymidylate kinase (tmk)	dTMP phosphorylation by ATP	dTDP binding	TMK + dTDP = TMK.dTDP	Michaelis constant (Km)	18	µM	calculated	calculated from other NTP and NDP affinities	-
thymidylate kinase (tmk)	dTMP phosphorylation by ATP	ADP binding	TMK + ADP = TMK.ADP	Michaelis constant (Km)	24	µM	calculated	calculated from other NTP and NDP affinities	-
thymidylate kinase (tmk)	dTMP phosphorylation by dATP	dATP binding	TMK + dATP = TMK.dATP	Michaelis constant (Km)	53	µM	calculated from literature	Calculated from (Munier-Lehmann, 2001.) 76% of ATP	-

enzyme	catalysed reaction	reaction step	equation	parameter name	parameter value	parameter dimension	from literature or calculated	note	reference
thymidylate kinase (tmk)	dTMP phosphorylation by dATP	dTMP phosphorylation by dATP	TMK.dTMP.dATP = TMK.dTDP.dADP	kcat	10,5	1/s	calculated from literature	Based on (Munier-Lehmann, 2001.), calculated using reaction K'	-
thymidylate kinase (tmk)	dTMP phosphorylation by dATP	dTMP phosphorylation by dATP reverse	TMK.dTMP.dATP = TMK.dTDP.dADP	kcat	5,4	1/s	calculated from literature	Based on (Munier-Lehmann, 2001.), calculated using reaction K'	-
thymidylate kinase (tmk)	dTMP phosphorylation by dATP	dADP binding	TMK + dADP = TMK.dADP	Michaelis constant (Km)	32	µM	calculated		-
thymidylate kinase (tmk)		dUDP binding	TMK + dUDP = TMK.dUDP	Michaelis constant (Km)	2500	µM	literature		(Tourneux *és mtsai.*, 1998)
thymidylate kinase (tmk)	dTMP phosphorylation by dGTP	dGTP binding	TMK + dGTP = TMK.dGTP	Michaelis constant (Km)	114	µM	calculated from literature	Calculated from (Munier-Lehmann, 2001.) 35% of ATP	-
thymidylate kinase (tmk)	dTMP phosphorylation by dGTP	dTMP phosphorylation by dGTP	TMK.dTMP.dGTP = TMK.dTDP.dGDP	kcat	10,5	1/s	calculated	Based on (Munier-Lehmann, 2001.)	-
thymidylate kinase (tmk)	dTMP phosphorylation by dGTP	dTMP phosphorylation by dGTP reverse	TMK.dTMP.dGTP = TMK.dTDP.dGDP	kcat	16,4	1/s	calculated	Based on (Munier-Lehmann, 2001.), calculated using reaction K'	-
thymidylate kinase (tmk)	dTMP phosphorylation by dGTP	dGDP binding	TMK + dGDP = TMK.dGDP	Michaelis constant (Km)	211	µM	calculated	calculated from other NTP and NDP affinities	-
thymidylate kinase (tmk)	dTMP phosphorylation by CTP	CTP binding	TMK + CTP = TMK.CTP	Michaelis constant (Km)	167	µM	calculated from literature	Calculated from (Munier-Lehmann, 2001.) 24% of ATP	-
thymidylate kinase (tmk)	dTMP phosphorylation by CTP	dTMP phosphorylation by CTP	TMK.dTMP.CTP = TMK.dTDP.CDP	kcat	10,5	1/s	calculated	Based on (Munier-Lehmann, 2001.)	-
thymidylate kinase (tmk)	dTMP phosphorylation by CTP	dTMP phosphorylation by CTP reverse	TMK.dTMP.CTP = TMK.dTDP.CDP	kcat	5,4	1/s	calculated	Based on (Munier-Lehmann, 2001.), calculated using reaction K'	-

enzyme	catalysed reaction	reaction step	equation	parameter name	parameter value	parameter dimension	from literature or calculated	note	reference
thymidylate kinase (tmk)	dTMP phosphorylation by CTP	CDP binding	TMK + CTP = TMK.CTP	Michaelis constant (Km)	100	µM	calculated	calculated from other NTP and NDP affinities	-
nucleotide diphosphate kinase (ndk)	NDK phosphorylation by ATP	ATP binding	NDK + ATP = NDK.ATP	Michaelis constant (Km)	22	mM	literature (S.cerevisiae)		(Jeudy, Claverie és Abergel, 2006)
nucleotide diphosphate kinase (ndk	NDK phosphorylation by ATP	Phosphorylation by ATP	NDK.ATP = NDK-P.ADP	kcat	130	mM/min	literature (S.cerevisiae)		
nucleotide diphosphate kinase (ndk	NDK phosphorylation by ATP	Phosphorylation by ATP reverse	NDK.ATP = NDK-P.ADP	kcat	170	mM/min	literature (S.cerevisiae)		
nucleotide diphosphate kinase (ndk	NDK phosphorylation by ATP	ADP binding	NDK-P.ADP = NDK-P + ADP	Michaelis constant (Km)	0,03	mM	literature (S.cerevisiae)		
nucleotide diphosphate kinase (ndk	NDK phosphorylation by GTP	GTP binding	NDK + GTP = NDK.GTP	Michaelis constant (Km)	0,15	mM	literature (S.cerevisiae)		
nucleotide diphosphate kinase (ndk	NDK phosphorylation by GTP	Phosphorylation by GTP	NDK.GTP = NDK-P.GDP	kcat	268	mM/min	literature (S.cerevisiae)	calculated from other NTP and NDP affinities	
nucleotide diphosphate kinase (ndk	NDK phosphorylation by GTP	Phosphorylation by GTP reverse	NDK.GTP = NDK-P.GDP	kcat	350	mM/min	literature (S.cerevisiae)		
nucleotide diphosphate kinase (ndk	NDK phosphorylation by GTP	GDP binding	NDK-P.GDP = NDK-P + GDP	Michaelis constant (Km)	1,5	mM	literature (S.cerevisiae)	calculated from other NTP and NDP affinities	
nucleotide diphosphate kinase (ndk	NDK phosphorylation by CTP	CTP binding	NDK + CTP = NDK.CTP	Michaelis constant (Km)	0,1	mM	literature (S.cerevisiae)		
nucleotide diphosphate kinase (ndk	NDK phosphorylation by CTP	Phosphorylation by CTP	NDK.CTP = NDK-P.CDP	kcat	220	mM/min	literature (S.cerevisiae)		
nucleotide diphosphate kinase (ndk	NDK phosphorylation by CTP	Phosphorylation by CTP reverse	NDK.CTP = NDK-P.CDP	kcat	83	mM/min	literature (S.cerevisiae)		

enzyme	catalysed reaction	reaction step	equation	parameter name	parameter value	parameter dimension	from literature or calculated	note	reference
nucleotide diphosphate kinase (ndk	NDK phosphorylation by CTP	CDP binding	NDK-P.CDP = NDK-P + CDP	Michaelis constant (Km)	0,3	mM	literature (S.cerevisiae)		
nucleotide diphosphate kinase (ndk	NDK phosphorylation by UTP	UTP binding	NDK + UTP = NDK.UTP	Michaelis constant (Km)	0,14	mM	literature (S.cerevisiae)		
nucleotide diphosphate kinase (ndk	NDK phosphorylation by UTP	Phosphorylation by UTP	NDK.UTP = NDK-P.UDP	kcat	400	mM/min	literature (S.cerevisiae)		
nucleotide diphosphate kinase (ndk	NDK phosphorylation by UTP	Phosphorylation by UTP reverse	NDK.UTP = NDK-P.UDP	kcat	75	mM/min	literature (S.cerevisiae)		
nucleotide diphosphate kinase (ndk	NDK phosphorylation by UTP	UDP binding	NDK-P.UDP = NDK-P + UDP	Michaelis constant (Km)	0,69	mM	literature (S.cerevisiae)		
nucleotide diphosphate kinase (ndk	NDK phosphorylation by dATP	dATP binding	NDK + dATP = NDK.dATP	Michaelis constant (Km)	0,13	mM	literature (S.cerevisiae)	calculated from other NTP and NDP affinities	
nucleotide diphosphate kinase (ndk	NDK phosphorylation by dATP	Phosphorylation by dATP	NDK + dATP = NDK.dATP	kcat	139	mM/min	literature (S.cerevisiae)	calculated from other NTP and NDP affinities	
nucleotide diphosphate kinase (ndk	NDK phosphorylation by dATP	Phosphorylation by dATP reverse	NDK + dATP = NDK.dATP	kcat	40	mM/min	literature (S.cerevisiae)		
nucleotide diphosphate kinase (ndk	NDK phosphorylation by dATP	dADP binding	NDK + dATP = NDK.dATP	Michaelis constant (Km)	0,5	mM	literature (S.cerevisiae)	calculated from other NTP and NDP affinities	
nucleotide diphosphate kinase (ndk	NDK phosphorylation by dCTP	dCTP binding	NDK + dCTP = NDK.dCTP	Michaelis constant (Km)	0,17	mM	literature (S.cerevisiae)		
nucleotide diphosphate kinase (ndk	NDK phosphorylation by dCTP	Phosphorylation by dCTP	NDK-P.dCDP = NDK.dCTP	kcat	380	mM/min	literature (S.cerevisiae)		
nucleotide diphosphate kinase (ndk	NDK phosphorylation by dCTP	Phosphorylation by dCTP reverse	NDK-P.dCDP = NDK.dCTP	kcat	110	mM/min	literature (S.cerevisiae)		

enzyme	catalysed reaction	reaction step	equation	parameter name	parameter value	parameter dimension	from literature or calculated	note	reference
nucleotide diphosphate kinase (ndk	NDK phosphorylation by dCTP	dCDP binding	NDK-P.dCDP = NDK-P + dCDP	Michaelis constant (Km)	0,4	mM	literature (S.cerevisiae)		
nucleotide diphosphate kinase (ndk	NDK phosphorylation by dGTP	dGTP binding	NDK + dGTP = NDK.dGTP	Michaelis constant (Km)	0,02	mM	literature (S.cerevisiae)		
nucleotide diphosphate kinase (ndk	NDK phosphorylation by dGTP	Phosphorylation by dGTP	NDK-P.dGDP = NDK.dGTP	kcat	132	mM/min	literature (S.cerevisiae)		
nucleotide diphosphate kinase (ndk	NDK phosphorylation by dGTP	Phosphorylation by dGTP reverse	NDK-P.dGDP = NDK.dGTP	kcat	38	mM/min	literature (S.cerevisiae)		
nucleotide diphosphate kinase (ndk	NDK phosphorylation by dGTP	dGDP binding	NDK-P.dGDP = NDK-P + dGDP	Michaelis constant (Km)	0,22	mM	literature (S.cerevisiae)		
nucleotide diphosphate kinase (ndk	NDK phosphorylation by dTTP	dTTP binding	NDK + dTTP = NDK.dTTP	Michaelis constant (Km)	0,11	mM	literature (S.cerevisiae)		
nucleotide diphosphate kinase (ndk	NDK phosphorylation by dTTP	Phosphorylation by dTTP	NDK-P.dTDP = NDK.dTTP	kcat	330	mM/min	literature (S.cerevisiae)		
nucleotide diphosphate kinase (ndk	NDK phosphorylation by dTTP	Phosphorylation by dTTP reverse	NDK-P.dTDP = NDK.dTTP	kcat	105	mM/min	literature (S.cerevisiae)		
nucleotide diphosphate kinase (ndk	NDK phosphorylation by dTTP	dTDP binding	NDK-P.dTDP = NDK-P + dTDP	Michaelis constant (Km)	0,37	mM	literature (S.cerevisiae)		
nucleotide diphosphate kinase (ndk	NDK phosphorylation by dUTP	dUTP binding	NDK + dUTP = NDK.dUTP	Michaelis constant (Km)	0,13	mM	literature (S.cerevisiae)		
nucleotide diphosphate kinase (ndk	NDK phosphorylation by dUTP	Phosphorylation by dUTP	NDK-P.dUDP = NDK.dUTP	kcat	8600	mM/min	literature (S.cerevisiae)		
nucleotide diphosphate kinase (ndk	NDK phosphorylation by dUTP	Phosphorylation by dUTP reverse	NDK-P.dUDP = NDK.dUTP	kcat	90	mM/min	literature (S.cerevisiae)		

enzyme	catalysed reaction	reaction step	equation	parameter name	parameter value	parameter dimension	from literature or calculated	note	reference
nucleotide diphosphate kinase (ndk	NDK phosphorylation by dUTP	dUDP binding	NDK-P.dUDP = NDK-P + dUDP	Michaelis constant (Km)	0,53	mM	literature (S.cerevisiae)		
Thymidylate synthase (thyA)	dTMP synthesys	dUMP binding	ThyA + dUMP = ThyA.dUMP	Michaelis constant (Km)	4,1	µM	literature	-	(Reyes *és mtsai.*, 1998)
Thymidylate synthase (thyA)	dTMP synthesys	mTHF binding	ThyA + mTHF = ThyA.mTHF	Michaelis constant (Km)	13,6	µM	literature	-	
Thymidylate synthase (thyA)	dTMP synthesys	dTMP synthesys	ThyA.dUMP.mTHF -> ThyA + dTMP + DHF	kcat	8,8	1/s	literature	-	
dUTPase (dut)	dUMP formation from dUTP	dUTP binding	dUTP + DUT = dUTP.DUT	Michaelis constant (Km)	0.5	µM	literature	-	(Barabás *és mtsai.*, 2004)
dUTPase (dut)	dUMP formation from dUTP	dUMP formation	DUT.dUTP -> DUT + dUMP	kcat	11	1/s	literature	-	
dCTP deaminase (dcd)	dCTP deamination to dUTP	dCTP binding	DCD + dCTP = DCD.dCTP	S0,5	66	µM	literature	The addition of 100 µM dTTP increased the S0.5 to values of 168 ± 8 µM	(Johansson *és mtsai.*, 2007; Thymark *és mtsai.*, 2008)
dCTP deaminase (dcd)	dCTP deamination to dUTP	dUTP formation	DCD.dCTP -> dUTP	kcat	1,24	1/s	literature		
dCTP deaminase (dcd)	dCTP deamination to dUTP	dUTP formation	DCD.dCTP -> dUTP	Hill coefficience	1,5		literature	The addition of 100 µM dTTP increased the Hill coefficient for dCTP to 3.3	
dCTP deaminase (dcd)	dCTP deamination to dUTP	dTTP binding	DCD + dTTP = Inc_DCD	Kd	35	µM	literature		
ribonucleotide reductase (rnr)	RNR complex formation	Rnr formation from alpha and beta subunits	RNRa + RNRb = RNR	affinity (Kd)	0,34-0,41	uM	literature data	affinity of the a2 and b2 subunits for each other is weak (~0.4 mM) in the absence of effectors, whereas the binding of a	(Hassan *és mtsai.*, 2008; Zimanyi *és mtsai.*, 2016)

enzyme	catalysed reaction	reaction step	equation	parameter name	parameter value	parameter dimension	from literature or calculated	note	reference
								complementary substrate/specificity effector pair increases the affinity of the class Ia RNR subunits fivefold	
ribonucleotide reductase (rnr)	RNR complex formation	Rnr activation via ATP binding	RNR + ATP = Act_RNR	Km	80	uM	literature		(Ormö és Sjöberg, 1990)
ribonucleotide reductase (rnr)		rnr inhibition via dATP binding	RNR + dATP = InAct_RNR	Km	0,43	uM	literature		(Ormö és Sjöberg, 1990)
ribonucleotide reductase (rnr)	dNDP production with dTTP activator	dTTP binding	Act_RNR + dTTP = Act_RNR.dTTP	Km	1,9	uM	literature		(Ormö és Sjöberg, 1990)
ribonucleotide reductase (rnr)	dCDP production with dTTP activator	CDP binding	Act_RNR.dTTP + CDP = Act_RNR.dTTP.CDP	Km	50	uM	literature		(Larson és Reichard, 1966)
ribonucleotide reductase (rnr)	dCDP production with dTTP activator	CDP reduction	Act_RNR.dTTP.CDP -> Act_RNR + dTTP + dCDP	specific activity	1950	nmol/min/mg	calculated	measured to dATP activation	(Zimanyi *és mtsai.*, 2016)
ribonucleotide reductase (rnr)	dGDP production with dTTP activator	GDP binding	Act_RNR.dTTP + GDP = Act_RNR.dTTP.GDP	Km	25	uM	literature		(Ormö és Sjöberg, 1990)
ribonucleotide reductase (rnr)	dGDP production with dTTP activator	GDP reduction	Act_RNR.dGTP.GDP -> Act_RNR + dGTP + dGDP	specific activity	1530	nmol/min/mg	calculated	measured to dTTP activation	(Zimanyi *és mtsai.*, 2016)
ribonucleotide reductase (rnr)	dADP production with dTTP activator	ADP binding	Act_RNR.dTTP + ADP = Act_RNR.dTTP.ADP	Km	30	uM	literature		(Larsson és Reichard, 1966)
ribonucleotide reductase (rnr)	dADP production with dTTP activator	ADP reduction	Act_RNR.dTTP.ADP -> Act_RNR + dTTP + dADP	specific activity	1200	nmol/min/mg	calculated	measured to dGTP activation	(Zimanyi *és mtsai.*, 2016)
ribonucleotide reductase (rnr)	dUDP production with dTTP activator	UDP binding	Act_RNR.dTTP + UDP = Act_RNR.dTTP.UDP	Km	220	uM	literature		(Larson és Reichard, 1966)

enzyme	catalysed reaction	reaction step	equation	parameter name	parameter value	parameter dimension	from literature or calculated	note	reference
ribonucleotide reductase (rnr)	dUDP production with dTTP activator	UDP reduction	Act_RNR.dTTP.UDP -> Act_RNR + dTTP + dUDP	specific activity	2600	nmol/min/mg	calculated	measured to dATP activation	(Zimanyi *és mtsai.*, 2016)
ribonucleotide reductase (rnr)	dNDP production with dGTP activator	dGTP binding	Act_RNR + dGTP = Act_RNR.dGTP	Km	0,77	uM	literature		(Ormö és Sjöberg, 1990)
ribonucleotide reductase (rnr)	dADP production with dGTP activator	ADP binding	Act_RNR.dGTP + ADP = Act_RNR.dGTP.ADP	Km	30	uM	literature		(Larsson és Reichard, 1966)
ribonucleotide reductase (rnr)	dADP production with dGTP activator	ADP reduction	Act_RNR.dGTP.ADP -> Act_RNR + dGTP + dADP	specific activity	1200	nmol/min/mg	calculated	measured to dGTP activation	(Zimanyi *és mtsai.*, 2016)
ribonucleotide reductase (rnr)	dNDP production with dATP activator	dATP binding	Act_RNR + dATP = Act_RNR.dATP	Km	6	uM	literature	allosteric activator	(Ormö és Sjöberg, 1990)
ribonucleotide reductase (rnr)	dCDP production with dATP activator	CDP binding	Act_RNR.dATP + CDP = Act_RNR.dATP.CDP	Km	50	uM	literature		(Larson és Reichard, 1966)
ribonucleotide reductase (rnr)	dCDP production with dATP activator	CDP reduction	Act_RNR.dATP.CDP -> dCDP + dATP + Act_RNR	specific activity	1950	nmol/min/mg	literature	measured to dATP activation	(Zimanyi *és mtsai.*, 2016)
ribonucleotide reductase (rnr)	dUDP production with dATP activator	UDP binding	Act_RNR.dATP + UDP = Act_RNR.dATP.UDP	Km	220	uM	literature		(Larson és Reichard, 1966)
ribonucleotide reductase (rnr)	dUDP production with dATP activator	UDP reduction	Act_RNR.dATP.UDP -> dUDP + dATP + Act_RNR	specific activity	2600	nmol/mg/min	literature	measured to dATP activation	(Zimanyi *és mtsai.*, 2016)

References

Barabás, O. *és mtsai.* (2004) „Enzyme Catalysis and Regulation : Structural Insights into the Catalytic Mechanism of Phosphate Ester Hydrolysis by dUTPase Structural Insights into the Catalytic Mechanism of Phosphate Ester Hydrolysis by dUTPase * and Bea”, *J. Biol. Chem.*, 279(41), o. 42907–42915. doi: 10.1074/jbc.M406135200.

Bernard, M. A. *és mtsai.* (2000) „Metabolic Functions of Microbial Nucleoside Diphosphate Kinases”, *Journal of Bioenergetics and Biomembranes*. Springer, 32(3), o. 259–267. doi: 10.1023/A:1005537013120.

Bucurenci, N. *és mtsai.* (1996) „CMP Kinase from Escherichia coli Is Structurally Related to Other Nucleoside Monophosphate Kinases”, *Journal of Biological Chemistry*. American Society for Biochemistry and Molecular Biology, 271(5), o. 2856–2862. doi: 10.1074/jbc.271.5.2856.

Hassan, A. Q. *és mtsai.* (2008) „Methodology To Probe Subunit Interactions in Ribonucleotide Reductases †”, *Biochemistry*. American Chemical Society, 47(49), o. 13046–13055. doi: 10.1021/bi8012559.

Hible, G. *és mtsai.* (2006) „Unique GMP-binding site in Mycobacterium tuberculosis guanosine monophosphate kinase”, *Proteins: Structure, Function and Genetics*, 62(2), o. 489–500. doi: 10.1002/prot.20662.

Holmes, R. K. és Singer, M. F. (1973) „Purification and characterization of adenylate kinase as an apparent adenosine triphosphate-dependent inhibitor of ribonuclease II in Escherichia coli.”, *Journal of Biological Chemistry*, 248(6), o. 2014–2021.

Jeudy, S., Claverie, J. M. és Abergel, C. (2006) „The nucleoside diphosphate kinase from mimivirus: A peculiar affinity for deoxypyrimidine nucleotides”, *Journal of Bioenergetics and Biomembranes*, 38(3–4), o. 247–254. doi: 10.1007/s10863-006-9045-y.

Johansson, E. *és mtsai.* (2007) „Regulation of dCTP deaminase from Escherichia coli by nonallosteric dTTP binding to an inactive form of the enzyme”, *FEBS Journal*, 274(16), o. 4188–4198. doi: 10.1111/j.1742-4658.2007.05945.x.

Larson, A. és Reichard, P. (1966) *Enzymatic Synthesis of Deoxyribonucleotides IX. ALLOSTERIC EFFECTS IN THE REDUCTION OF PYRIMIDINE RIBONUCLEOTIDES BY THE RIBONUCLEOSIDE DIPHOSPHATE REDUCTASE SYSTEM OF ESCHERICHIA COLT"*, *THE JOURNAL OF BIOLOGICAL CHEYISTRY*. Elérhető: http://www.jbc.org/ (Elérés: 2020. július 1.).

Larsson, A. és Reichard, P. (1966) *Enzymatic Synthesis of Deoxyribonucleotides X. REDUCTION OF PURINE RIBONUCLEOTIDES; ALLOSTERIC BEHAVIOR AND SUBSTRATE SPECIFICITY OF THE ENZYME SYSTEM FROM ESCHERICHIA COLI B**, *THE JOURNAL OF BIOLCKXCAL CHEMIEWRY*. Elérhető: https://www.jbc.org/content/241/11/2540.full.pdf (Elérés: 2020. július 1.).

Munier-Lehmann, H. *és mtsai.* (2001) „Thymidylate kinase of Mycobacterium tuberculosis: A chimera sharing properties common to eukaryotic and bacterial enzymes”, *Protein Science*, 10(6), o. 1195–1205. doi: 10.1110/ps.45701.

Oeschger, M. P. (1978) „[63] Guanylate kinase from Escherichia coli B”, in *Methods in Enzymology*, o. 473–482. doi: 10.1016/S0076-6879(78)51065-3.

Ormö, M. és Sjöberg, B. M. (1990) „An ultrafiltration assay for nucleotide binding to ribonucleotide reductase”, *Analytical Biochemistry*, 189(1), o. 138–141. doi: 10.1016/0003-2697(90)90059-I.

Reyes, C. L. *és mtsai.* (1998) „Inactivity of N229A thymidylate synthase due to water-mediated effects: Isolating a late stage in methyl transfer”, *Journal of Molecular Biology*, 284(3), o. 699–712. doi: 10.1006/jmbi.1998.2205.

Thymark, M. *és mtsai.* (2008) „Mutational analysis of the nucleotide binding site of Escherichia coli dCTP deaminase”, *Archives of Biochemistry and Biophysics*, 470(1), o. 20–26. doi: 10.1016/j.abb.2007.10.013.

Tourneux, L. *és mtsai.* (1998) „Substitution of an alanine residue for glycine 146 in TMP kinase from Escherichia coli is responsible for bacterial hypersensitivity to bromodeoxyuridine”, *Journal of Bacteriology*, 180(16), o. 4291–4293.

Zimanyi, C. M. *és mtsai.* (2016) „Molecular basis for allosteric specificity regulation in class ia ribonucleotide reductase from Escherichia coli”, *eLife*, 5(JANUARY2016), o. 1–23. doi: 10.7554/eLife.07141.